OSLOMET

Master's Thesis

Master´s degree in Biomedicine

November 2021

Establishment and characterization of cell lines to study the proxymitome of the Centrosome and Spindle Pole-associated protein 1

Christa Irakoze

MABIO5900

60 ECTS

Faculty of Health Sciences
OSLO METROPOLITAN UNIVERSITY
STORBYUNIVERSITETET

Establishment and characterization of cell lines to study the proxymitome of the Centrosome and Spindle Pole-associated protein 1

by

Christa Irakoze

Main supervisor: Sebastian Patzke

Co-supervisor: Trond Stokke

Master of Biomedicine

60 ECTS

Institute for Cancer Research

Department of Radiation Biology

Centrosome & Cell Division Cycle Project Group

Oslo University Hospital, Norwegian Radium Hospital

Faculty of Health Sciences

Department of Life Sciences and Health

OsloMet - Oslo Metropolitan University

November 2021

OSLOMET

OSLO METROPOLITAN UNIVERSITY
STORBYUNIVERSITETET

Oslo universitetssykehus
Radiumhospitalet

Acknowledgements

The work in this master thesis was performed at the Norwegian Radium Hospital in the Radiation Biology Department as part of the Centrosome and Cell Division Cycle Project Group from August 2020 to November 2021.

I would first of all like to thank my main supervisor, Sebastian for his guidance through this year and for proofreading this thesis. I would also like to thank Kari-Anne for all the help in the lab and protocols, it was much appreciated. Furthermore, I would like to thank Sania for the help in the virus lab, thank you for your guidance in the virus lab and for answering all my questions.

I am very grateful for allowing me to be part of the group, I have learned so much during this year. My family has been a big support throughout this time, I am so grateful for them being there for me.

Abstract

Background: The predominantly expressed isoform of *CSPP1*, CSPP-L, is a centrosomal and Centriolar satellite protein with functions in microtubule organization in cell division and cilia formation. CSPP-L dose and microtubule organizing activity need to be tightly regulated. Its over-expression manifests in multipolar spindle assembly and cell division failure, which is a hallmark of cancer. Its depletion or functional loss manifests in defective cilia assembly and signaling, and is also an underlying cause of a human ciliopathy. The mechanism controlling CSPP-L's activity and localization are not understood.

Aim: The aim of this project was to generate and characterize cell lines expressing a miniTurboID-CSPP-L fusion protein. The miniTurboID-tag encodes for a promiscuous biotin-ligase, which can be exploited to label proteins that are proximal to CSPP-L in a living cell.

Material and methods: Molecular genetics and cell biological techniques were used to construct and produce lentiviral particles to stably introduce a miniTurboID-CSPP-L expressing cassette into hTERT-RPE1 cells. Immunofluorescence microscopy and Western blot were used to characterize these cell lines. The localization pattern of miniTurboID-CSPP-L and biotinylation-activity were studied by immunofluorescence microscopy, and biotinylated proteins were tried isolated using streptavidin-agarose.

Results: Cell lines expressing miniTurboID-CSPP-L protein were constructed. The fusion protein localizes to and rapidly biotinylates proteins at Centriolar satellites, the centrosome, and mitotic spindle. Unexpectedly, in initial analyses the fusion protein was not detected at primary cilia. This should be studied further. Fluorescens microscopy confirmed biotinylation of proteins within 5-10 minutes after addition of biotin. Preparative extraction of biotinylated proteins required further optimization.

Conclusion: We successfully generated hTERT-RPE1 cells expressing CSPP-L that can be used to determine its proxymitome in living cells at high temporal resolution. The N-terminally tagged fusion protein localizes to centrosomes and Centriolar satellites. Further work is warranted to investigate the potential perturbance of CSPP-L's ciliary function/localization by fusion to the miniTurboID-tag.

Sammendrag

Bakgrunn: CSPP-L er et centrosomalt og Centriolært satellitt protein som lokaliserer til den mitotiske spindelen under mitosen og til det primære cilium i serum sultede celler. Overutrykk av CSPP-L er assosiert med kreft, og fører til avvik under celledelig og dannelse av multipolare spindeler. Når CSPP-L ikke uttrykkes eller er mutert fører dette til feil i dannelse og funksjon av cilia, dette er igjen en underliggende årsak for ciliopati.

Mål: Målet med dette prosjektet var å etablere cellelinjer som uttrykker miniTurboID-CSPP-L fusjonsproteinet. miniTurboID-tagen koder for en biotin ligase som kan brukes til å merke proteiner som er i nærheten av fusjonsproteinet i levende celler.

Material og metode: Immunofluorescens mikroskopi og Western blot ble benyttet til å studere lokalisering av miniTurboID-CSPP-L. Biotinylerte proteiner ble også obsevert ved Immunofluorescens mikroskopi, deretter forsøkt isolert og ekstrahert med streptavidin-agarose kuler.

Resultater: miniTurboID-CSPP-L proteinet lokaliserte som forventet til centrosomet og Centriolære satelliter, men ble ikke detektert ved det primær ciliumet. Det ble også undersøkt om miniTurboID-CSPP-L biotinylerte proteiner. Resultatetene viste biotinylerte proteiner etter 5-10 min.

Konklusjon: Det ble laget celler som uttrykker miniTurboID-CSPP-L og som er i stand til å biotinylere proteiner i nærhet. Lokalisering av miniTurboID-CSPP-L til centrosomene og Centriolære satelliter ble validert, men lokalisering til det primær ciliumet må studeres videre.

Abbreviations

3D-SIM 3-Dimentional Structured Illumination Microscopy

ADP Adenosine diphosphate

ARMC9 Armadillo repeat Containing 9

ARL13B ADP Ribosylation Factor Like GTPase 13B

BioID Proximity-dependent biotin identification

BirA Bifunctional ligase/repressor BirA

BSA Bovine Serum Albumin

CCDC66 Coiled-Coil Domain Containing 66

CEP97 Centrosomal protein of 97 kDa

CEP104 Centrosomal protein of 104 kDa

CEP131 Centrosomal protein of 131 kDa

CEP164 Centrosomal protein of 164 kDa

CEP290 Centrosomal protein of 290 kDa

CP110 Centrosomal protein of 110 kDa

CS Centriolar satellites

CSPP1 Centrosome, spindle pole and cilia associated protein 1

CSPP-L Predominant isoform of CSPP1

DA Distal appendages

DAV Distal appendage vesicles

DMEM Dulbecco´s Modified Eagle Medium

DNA Deoxyribonucleic acid

EB3 Plus-end tracking protein

EHD1 EH domain-containg protein 1

FBS Fetal Bovine Serum

GTP Guanosine triphosphate

HEK293T Cell line; Human embryonic kidney

Hh Hedgehog

HRP Horseradish Peroxidase

hTERT-RPE1 Cell line; Human Telomerase Reverse Transcriptase immortalized - Retinal Pigment Epithelia 1

IFT Intraflagellar transport

JBTS Joubert syndrome

KIAA0556 Protein KIAA0556

KIF7 Kinesin-like protein KIF7

LentiX HEK293T cell line

MAP4 Microtubule Associated Protein 4

MAPs Microtubule -associated proteins

MIPs Microtubule interacting proteins

MKS Meckel-Gruber Syndrome

MTOC Microtubule-organizing center

MQH_2O Milli-Q water

PBS Phosphate buffered saline

PBS-AT PBS with added albumin and triton

PCM Pericentriolar material

PCV The primary ciliary vesicle

P/S Penicillin/Streptamycin

PVDF Polyvinylidene difluoride

Rab11 Ras-related protein Rab-11

Rab8 Ras-related protein Rab-8

SDS-PAGE Sodium dodecylsulfate polyacrylamide gel electrophoresis

SLS Senior-Løken syndrome

SMO Smoothened

TBST buffer tris buffered saline with Tween

TF Transition fiber

TOGARAM1 TOG Array Regulator of Axonemal Microtubules 1

TTBK2 Tau tubulin kinase 2

TZ Transition zone

γ-TuRC γ-tubulin ring complex

TABLE OF CONTENTS

1. Introduction

1.1 Centrosome and Microtubules

1.1.1 Centrosome

Centrosome function and structure

The centrosome functions as a microtubule organizing center (MTOC) in all animal cells. The non-membranous organelle is also involved in critical cellular processes such as cell division, polarity and motility. The centrosome consists of two microtubule-based structures called centrioles, where a mother centriole and the daughter centriole can be distinguished (1). The centrioles are embedded in an electron dense material called pericentriolar material (PCM), which contains γ-tubulin ring complexes and is important for microtubule nucleation and organization. The mature mother centriole acquires subdistal- and distal appendages, important for the mother centriole to function as microtubule anchoring center during interphase (subdistal appendages) and basal body for the primary cilium assembly (distal appendages) (2, 3). The centrioles are made of nine triplet microtubules that are arranged in a ring form. The triplet consists of a complete inner microtubules, the A-tubule, and two adjunct outer microtubules, the B- and the C-tubule. The nine triples are linked together by the A-C linkers. The distal ends of the centrioles consist only of doublet microtubules, since the C-tubule is early terminated and does not extend to the distal end of the centriole (4).

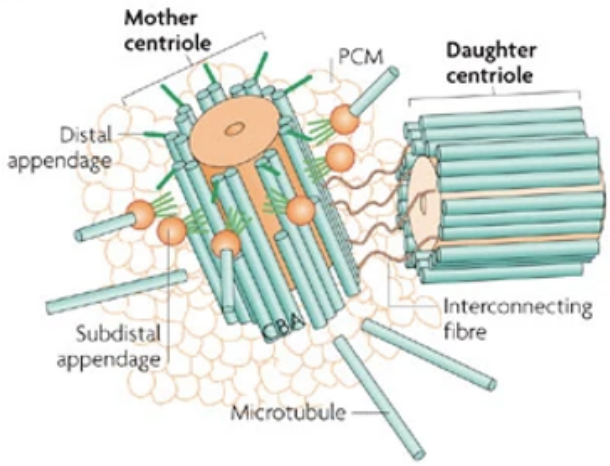

Figure 1*:* The centrosome structure. The mother centriole contains distal and subdistal appendages and the two centrioles are connected by an interconnecting fiber (7).

Centrosome duplication

The centrosome duplicates only once during the cell cycle. Centrosome duplication begins in S-phase when the pro-centriole is formed orthogonally positioned from the proximal end of each centriole (mother and daughter centriole) (5). The procentrioles are further elongated throughout the G_2-phase. The older centrioles with their respective daughters separate during the transition from the late G_2-phase to mitosis when the linker between them is dissolved. This happens after the centrioles have accumulated more PCM, which increased MTOC activity for spindle pole formation. Once the centrosomes have been separated, they can form the poles of the bipolar mitotic spindle and each new cell will then inherit one centrosome after the cell has completed mitosis and entered G_1-phase. Distal and subdistal appendages are now acquired, making the former daughter centriole to a mature mother centriole (6, 7).

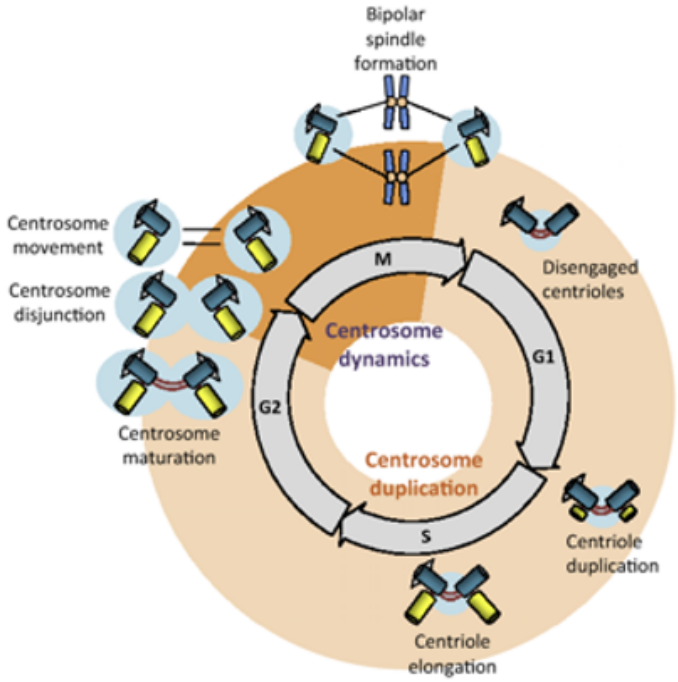

Figure 2: Centrosome duplication (8).

1.1.2 Microtubules

Microtubules are cytoskeletal filaments. They are involved in cellular processes such as cell migration, division and intracellular transport. During cell division, MTOC form the mitotic spindle which is responsible for the separation of the duplicated chromosomes to opposite sides of the cell when the two daughter cells are created (9, 10). Thirteen proto-filaments form a microtubule with a hollow, straw-shaped structure. Protofilaments are formed by a uniform heterodimer consisting of α-tubulin and β-tubulin. In most animal cells, microtubules are

nucleated from the MTOC in the perinuclear region which contains proteins that are implicated in microtubule nucleation and organization. Among these proteins is the γ-tubulin ring complex (γ-TuRC), which is the microtubule nucleation site at the minus end from where dimers of α and β-tubulin are added to form a microtubule (9).

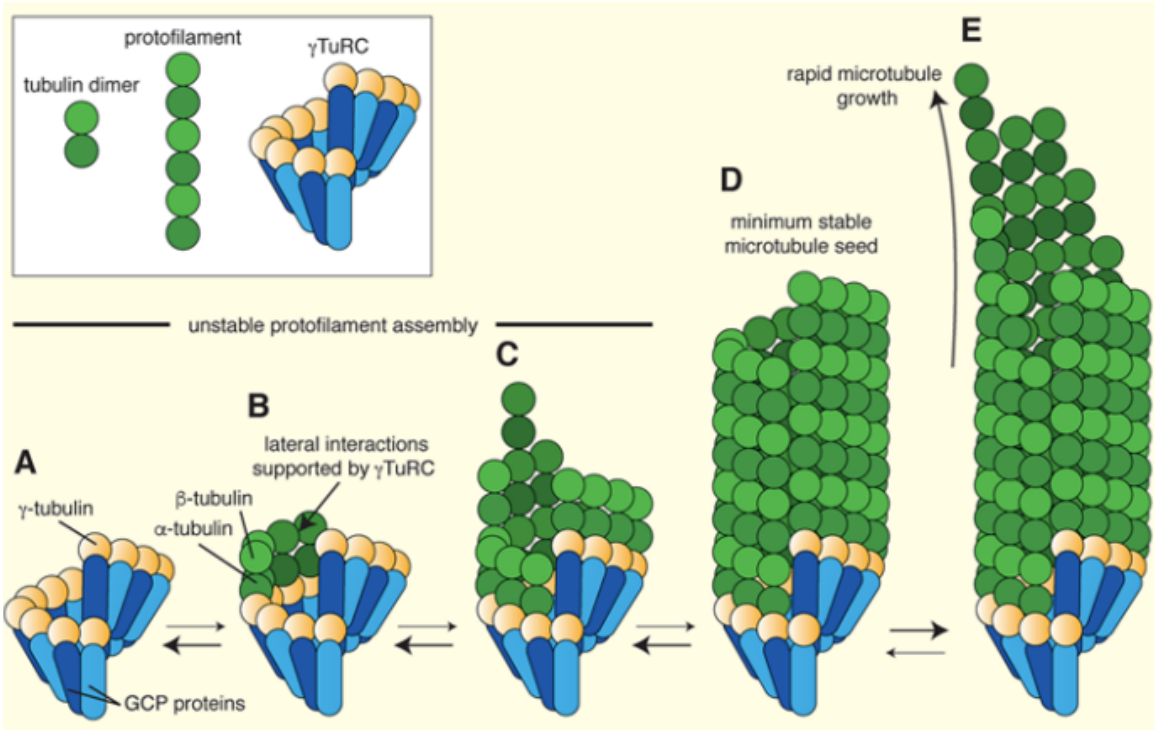

Figure 3: Microtubule nucleation from the γ-TuRC complex. The core γ-TuRC complex is composed of γ-tubulin and GCP proteins and is where the microtubule is nucleated. (11)

The microtubules are dynamic. They continuously cycle between growing (polymerization) and shrinking (depolymerization) phases. This phenomen is termed dynamic instability (12). Microtubule dynamics are regulated by microtubule associated proteins (MAPs). Microtubule plus-end binding proteins (EBs) are a particular class involved in controlling growth at the plus-end of the tubule. There are MAPs that have a stabilizing effect and other MAPs that have a destabilizing effect.

The microtubule plus-end tracking proteins (+TIPs) complex are an important group of MAPs. The +TIP protein complex is located on the plus-end of a growing microtubule and plays a role in regulating microtubule dynamic. They also participate in the interaction of microtubules with chromosome and the cell cortex in mitosis. The core of this complex is formed by the plus-end-binding proteins EB1, EB2 and EB3 (9, 13).

1.1.3 Centriolar satellites

Centriolar satellites (CS) are small electron-dense granules of about 70-100 nm in diameter. They were first identified in the late half of 1900s when a group of scientists was studying the centrosome structure (14) The cellular distribution of these satellites varies, it is cell type and differentiation dependent (15). The CS are clustered in the region near the mother centriole in ciliated cells, and CS dissolute during mitosis. Most of the CS located on microtubules are in movement towards the centrosome with the help of the motor protein dynein. CS proteins may function in mediating transport of both centriolar- and PCM-protein complexes from the cytoplasm to the centrosome along microtubules (16). When microtubules are depolymerized, CS are spread throughout the cytoplasm. CS also play a role in primary cilia assembly by delivering centriolar components or centrosomal components from the cytoplasm to the centrosome. The importance of CS proteins is underlined by the fact that mutations in genes encoding for satellite proteins or their regulating components are found causative for various human congenic disorders, including ciliopathies (17). So far, 223 CS proteins have been identified by affinity purification using PCM1 as the bait protein (15).

A.

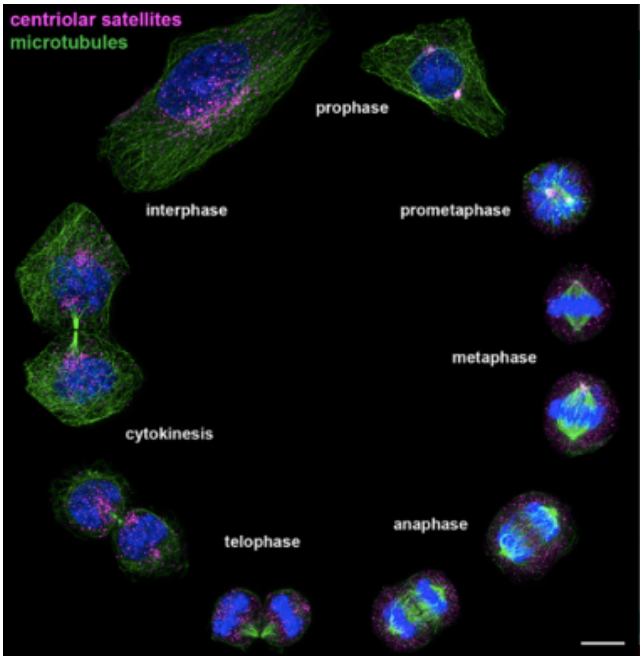

B.

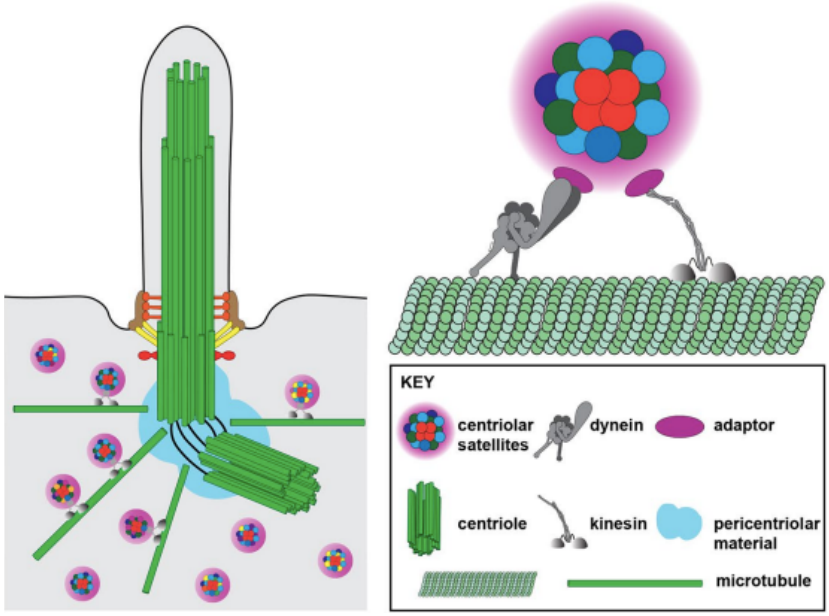

Figure 4: (A) Figure displaying localization of CS during the cell cycle. Human Hela cells were stained with anti-PCM1 for detection of CS (magenta), anti-α-tubulin for detection of microtubules (green) and DAPI for detection of DNA (blue). Scale bar is 10 µm. (B) Figure showing movement of satellites proteins around the centrosome and cilium in a microtubule and molecular motor-dependent manner. (15)

Pericentriolar material 1, PCM1 was the first identified satellite protein and has been accepted as a marker for CS (1). PCM1 is viewed as a fundamental component for other CS proteins. This is because when PCM1 is depleted or mutated the CS proteins are disassembled (17). As

stated above, so far 223 CS proteins have been identified by affinity purification using PCM1 as the bait protein. In addition, an extensive interactome of more than 600 proteins has been generated in proximity labelling studies using 21 further Centriolar satellite proteins as bait proteins (18). The function of CS proteins has to most extent been explored by loss-of-function studies, where PCM1 has been used as a satellite protein marker (19). CSPP1, CCDC66, CEP290 and CEP131 are some of the satellite proteins that have been recognized to be interacting with PCM1 (15, 18). The dynamic behavior of CS is still little understood but important for understanding how they function (20). The regulation of their assembly and disassembly represents a further research front in the field (1). Post-translational modifications are known to contribute to their regulations, but the modifying enzymes and up-stream regulatory mechanism(s) are not known.

1.2 Primary Cilium

1.2.1 Structure and function

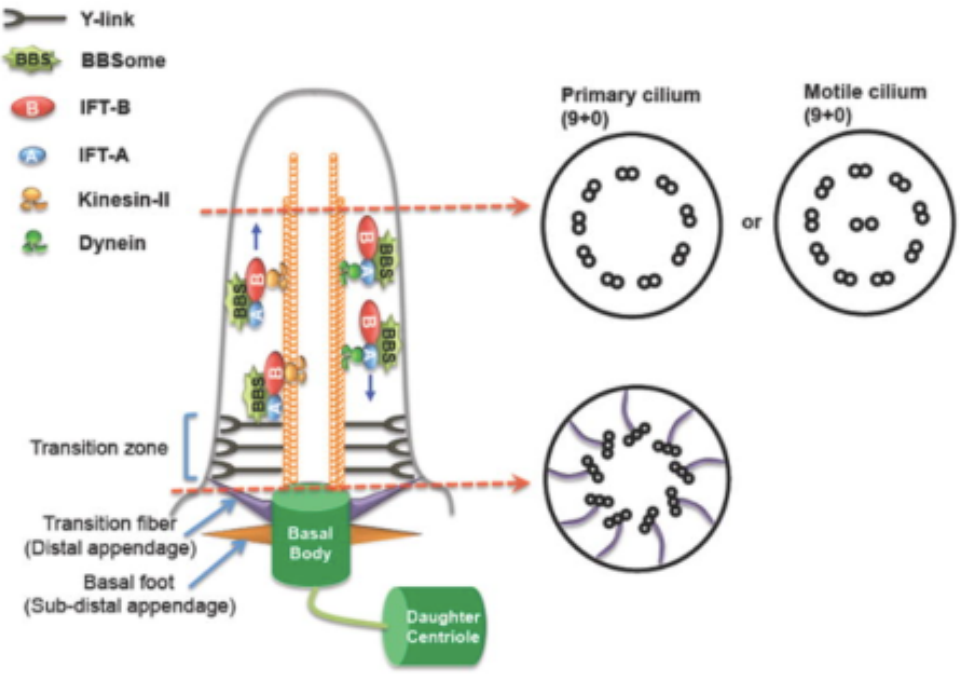

Figure 5: The primary cilium structure. The base of the cilium consist of the basal body and daughter centriole. The axoneme is extended from the basal body with a structure of nine doublet microtubules. (21)

The primary cilium is a non-motile sensory organelle (22). Primary cilia function as the cell´s antenna receiving signal from the extracellular environment and transmitting them to the cell

as part of the regulation, developmental and physiological processes of the cell (23, 24). Primary cilia are present in almost every cell in the body and are actively involved in signaling pathways such as Hedgehog (Hh)-signaling (25). Some cell types generate one or numerous motile cilia. These differ from the non-motile cilia by the formation of an additional pair of microtubules within the arrangement of the nine doublet microtubules that are extended from the centriole. The axoneme organization of non-motile cilia is denoted as (9+0) configuration, and that of motile cilia as (9+2) configuration (26). Motile cilia promote cell movement and fluid flow. Motor protein-driven sliding of the inner pair create the beating movement of the motile cilium (26).

As already mentioned, the ciliary axonemal structure consists of nine doublet microtubules that are composed of one complete tubule made of 13 proto-filaments, the A-tubule, and one incomplete tubule, the B-tubule, that is formed by 10 proto-filaments and closed by attachment to the A-tubule. The doublet microtubules transition into singlet A-tubules towards the distal end of the cilium when the B-tubule terminates. The microtubule minus end is anchored on the basal body while the plus-end of the microtubule is exposed to the ciliary lumen.

Microtubule-associated proteins (MAPs) act as motor proteins and regulate stability, dynamics and motility of microtubules. For example, CEP104, TOGARAM, ARMC9, CCDC66 and CSPP1 form an axonemal MAP complex (27). This complex is assumed responsible for the regulation of axoneme maintenance, stability, length and concomitantly impacts on ciliary Hh-signaling. Mutations in gene encoding these proteins have been linked to ciliopathies. CEP104, TOGARAM, ARMC9 and *CSPP1* have been linked to Joubert syndrome and CCDC66 to a retinopathy. The exact function of individual axonemal MAP complex members in microtubule regulation, as well as the crosstalk with the Hh-signaling pathway are not fully understood and topic of current investigations in several laboratories. The microtubule plus-end tracking proteins EB1 and EB3, MAP4 and a subset of ciliary kinesins are other ciliary MAPs that are known to regulate the length, stability and structure of cilium but are not associated with the aforementioned axonemal MAP complex (28).

Examples of further non-tubulin content that is associated with the primary cilium are microtubule inner proteins (MIPs). MIPs associate with the internal wall of microtubules as

well as proteins that float in the microtubule lumen. MIPs localize along the axoneme of the primary cilium (28).

The axoneme is an extension of the A-tubule and B-tubules of the mother centriole, which is transformed into a basal body (25). A mature cilium consists of a transition zone (TZ), axoneme and the tip-region of the cilium, all enclosed within a ciliary membrane. The primary cilium is anchored to the cell membrane through the distal appendages (DA) which are acquired by the mother centriole to function as a basal body. The DA are fibrous structures and are localized on the distal end of the mother centriole. DA matures into the transition fibers (TF) during the assembly of the cilium. The transition zone defines the border between the cell membrane and the ciliary membrane with their nine-bladed propeller like structures (23). The TF is the proximal part of the axoneme and is the part that contains Y-linkers. The Y-linkers connect the microtubules of the axoneme to the ciliary membrane. The part of the cilia which consist of the TF and the TZ is where cilia control what is transported to the cell or from the cell and that is also the part that separates the basal body from the ciliary axoneme (21, 24).

The region between the distal end of the axoneme and the ciliary membrane is called the ciliary tip, this is the site of dynamic growth and disassembly of the axoneme, remodeling of intraflagellar transport (IFT) trains and Hedgehog signaling (28). IFT trains is movement of anterograde and retrograde on the cilium axoneme. The IFT complexes are transported bi-directionally on the cilia axoneme to transport protein cargo to or from the basal body for the cilia assembly and maintenance (26, 29). The tip of the cilium is where the remodeling IFT for retrograde transport complex takes place, axoneme length is regulated and crucial components of the Hedgehog signaling pathway are localized and controlled (21, 24). The Hedgehog signaling pathways is critical for embryonic development and tissue homeostasis. Ciliary accumulation of the 7-pass transmembrane protein Smoothened (SMO) and GLI transcription factors is a key step in the activation of the Hedgehog signaling cascade. Loss of either CEP104 or CSPP1 has been reported to reduce ciliary accumulation of SMO, and loss of ARMC9 perturbed accumulation of GLI transitions factors at the ciliary tip upon activation of hedgehog signaling pathway (30).

1.2.2 Ciliogenesis

Ciliogenesis is the process of primary cilium assembly, which only occurs after the cell exited mitosis (31). Ciliation in cells, such as hTERT-RPE1 cells can be induced by serum withdrawal from the cell culture medium (32). Cells form cilia, either by the intracellular assembly pathway (axoneme assembly starts in cytoplasm) or the extracellular assembly pathway (axoneme assembly starts after attachment to cell membrane). hTERT-RPE1 cells use the intracellular pathway while epithelial cells use the extracellular pathway. Cilia formation is initiated by the accumulation of small cytoplasmic vesicles near the distal appendages (DA) located on the mother centriole. The nine axonemal triplet microtubule function as the template for the construction of the nine doublet axonemal tubules during the elongation of the cilia axoneme (33). These vesicles are transported by dynein or Myosin5a along the microtubules from the Golgi apparatus to the mother centriole. The pre-ciliary vesicle (PCV) is then formed when the distal appendage vesicles (DAV) dock and fuse at the mother centriole. Thereafter the PCV will fuse with multiple small vesicles, until covering the distal end of the mother centriole. The formation of the PCV triggers the removal of the so called capping complex from the distal end of the mother centriole, which in turn permits the elongation of the axoneme while surrounded by a double-membrane sheath that is developed from the PCV (34).

EH Domain Containing 1 (EHD1) is responsible for the transportation of vesicles to the mother centriole and is located on the preciliary membrane. The Rab11-Rab8 cascade is required for the formation of ciliary membrane. Rabin8, which is the guanine nucleotide exchange factor for Rab8, binds to rab11. The complex is then delivered to the centrosome in vesicles, where Rab8 is activated and the ciliary membrane assembly is promoted (35). ADP-ribosylation factor-like protein 13B (ARL13B) is a GTPase localized on the ciliary membrane and is involved in cilia formation and ciliary trafficking. Thereby ARL13B has been used as a ciliary membrane marker (34, 36).

Core components of the capping complex are CP110 and CEP97. The removal of CP110 and CEP97 from the distal part of the mother centriole is promoted by an enzyme called Tau Tubulin Kinase 2 (TTBK2) located on the distal end of the basal body. This step is required for the formation of the cilium. TTBK2 also promotes the recruitment of IFT-proteins which build the ciliary axoneme by mediating the transport of ciliary axonemal proteins. TTBK2 is recruited by the distal appendage protein CEP164. Both CP110 and CEP97 are negative

regulators of primary cilia formation, they prevent cilia formation in inappropriate stages of the cell cycle (37-39).

The transition zone (TZ) is formed after the removal of the cap proteins, and initiated when the axonemal microtubules can elongate (34). The extension of the ciliary axoneme and membrane is mediated by the IFT machinery (40). IFT proteins are important for the growth and maintenance of the cilia. IFT-proteins consist of IFT-A and IFT-B protein complexes. Both protein complexes play roles in ciliary trafficking. The IFT-A protein complex transports proteins from the tip to the base (retrograde) and is associated with the dynein-2 motor protein complex. The IFT-B protein complex transports proteins from base to tip (anterograde) and is associated with the kinesin-2 motor protein complex (29, 36).

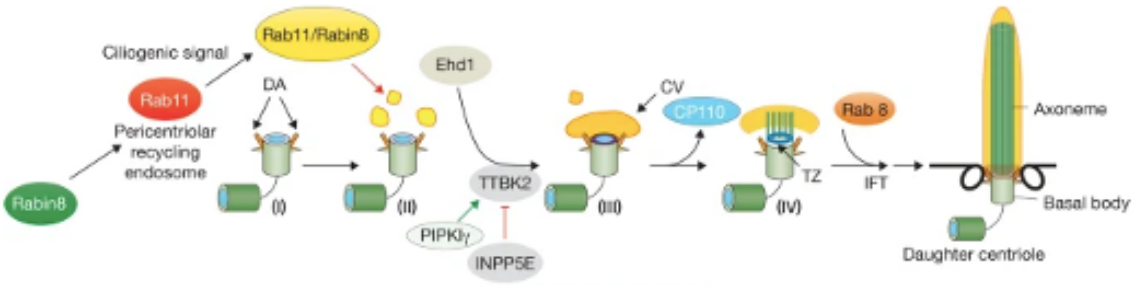

Figure 6: Events in the intracellular pathway of primary cilium assembly. (32)

1.3 Ciliopathies

Ciliopathies are a group of disorders that are caused by defective primary cilia formation or function (23, 41). Examples of ciliopathies are Joubert syndrome (JBTS), Senior-Løken syndrome (SLS) and Meckel-Gruber syndrome (MKS). These ciliopathies affect different organs such as the liver, brain and kidney.

Joubert syndrome is an autosomal recessive disorder. The characteristic of JBTS is the “Molar Tooth Sign”, a midbrain-hindbrain malformation (42). Affected individuals suffer from general developmental delay and intellectual disability. Most of the 39 identified proteins so far that are involved, are localized or play a role in the function of the transition zone of the primary cilium (43, 44). KIF7, KIAA0556, CSPP1, CEP104, ARMC9 and TOGARAM1 are the only Joubert syndrome-related proteins that are located to the tip of the cilia axoneme, defining them as a potential specific subgroup. The tip of the cilium is important for

trafficking of proteins. The cilium assembly is controlled on the base of the cilium and that is also where ciliary proteins are passaged (30). *CSPP1* is often mutated in Joubert syndrome and related diseases and account for 2-3% of reported cases (45).

JBTS is also manifested by a variety of other brain malfunction and abnormal breathing and eye movement. It has been shown that, small interfering RNA knockdown of CSPP1 lead to a decrease in number of ciliated Human Telomerase Reverse Transcriptase immortalized - Retinal Pigment Epithelia (hTERT-RPE) cells (46).

1.4 The Centrosome and Spindle-Pole associated Protein 1 gene (*CSPP1*)

1.4.1 Protein structure and function

CSPP1 encodes for two splice isoforms, CSPP and CSPP-L. These protein isoforms are involved in the microtubule organization and the cell cycle progression. CSPP-L is the larger and predominantly expressed isoform of *CSPP1*. The CSPP-L protein can be divided into three domains: N-terminal, mid-domain and C-terminal. Compared to the CSPP protein isoform, the CSPP-L transcript is driven by a different promoter. The transcript translates into a longer N-terminal domain as well as comprises an additional exon within the central coiled-coil domain-coding region (47). CSPP-L has a 294 amino acid longer N-terminal than the CSPP and an additional 51 amino acid long insertion located in the coiled-coil mid-domain. The *CSPP1* proteins have a tripartite domain structure, where the N-terminal and C-terminal is linked through an excessive coiled-coil domain-rich mid-domain. The N-terminal and the coiled-coil mid-domain comprise the microtubule-targeting domain and is required for the ciliary localization and localization on the centrosome (47, 48)

Figure 7: Protein structure of CSPP-L and CSPP. The CSPP-L contain additional amino acid, highlighted in grey (N-terminal). The bold bars are coiled-coil regions. (40)

CSPP-L is located to centrosomes throughout the cell cycle. Notably, CSPP-L gains additional affinity for specific microtubule assemblies in distinct cell cycle phase. During prophase to metaphase CSPP-L is decorating mitotic spindle microtubules and is relocated to the mid-spindle during anaphase, at which it is concentrated at the mid-body and cytokinetic bridge in telophase/cytokinesis. During interphase extra-centrosomal CSPP-L is localized to Centriolar satellites and concentrated at the MTOC (49). In ciliated cells, CSPP-L is localized to the basal body and its transition zone, decorates the ciliary axoneme and is prominently accumulated at the ciliary tip.

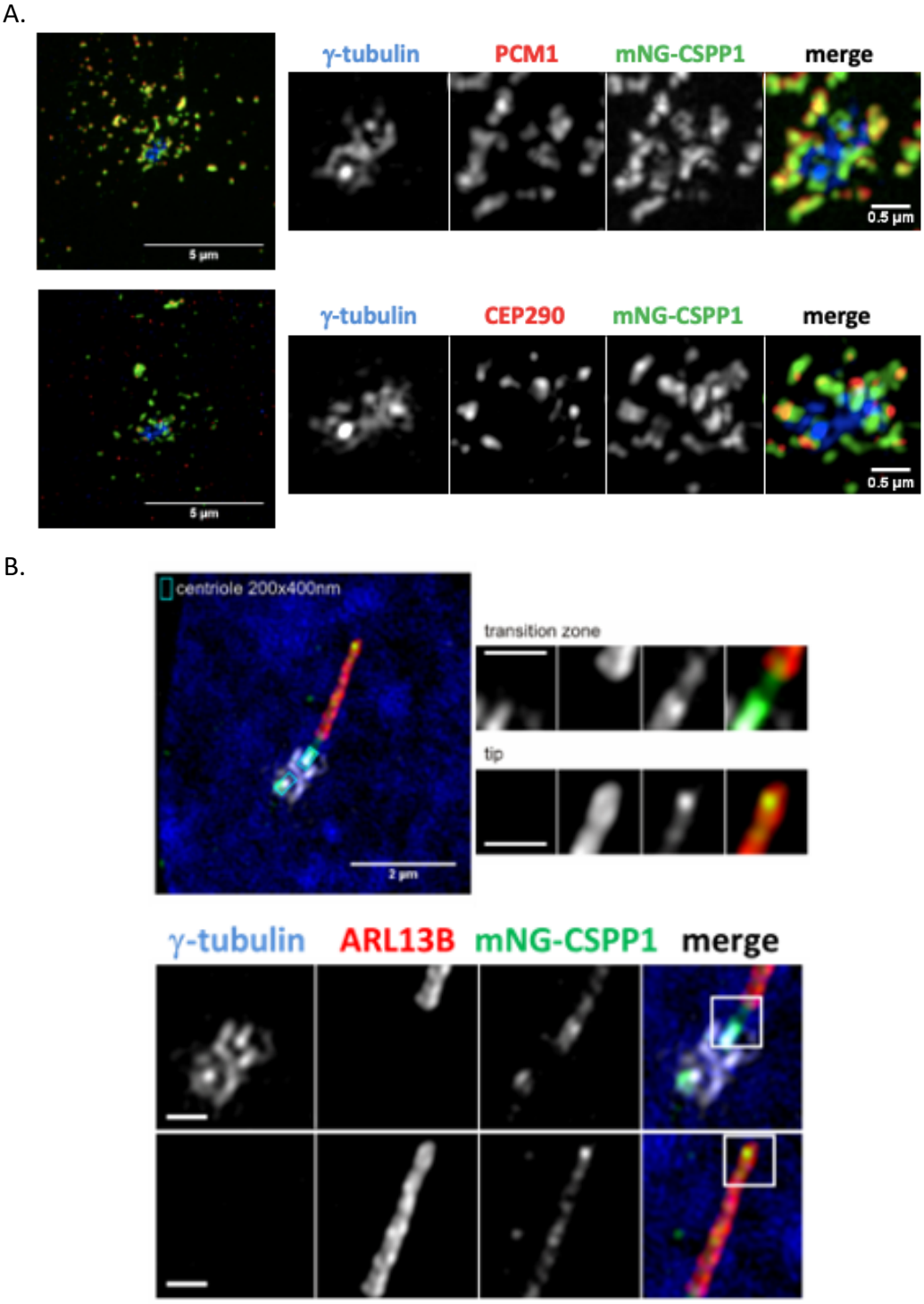

Figure 8: The previous master student, Sania Gilani, generated mNG-CSPP-L (here designated *CSPP1*) expressing cells and showed localization of the mNG-CSPP-L protein on primary cilium (B) (50). (A) Figure display 3D- Structured Illumination Microscopy (3D-SIM) images of mNG-CSPP-L localized on the centrosome. Images were generated by Sebastian Patzke (Department of Radiation Biology, Institute of cancer research (ICR), Oslo University Hospital (OUH)).

Earlier studies have shown defects in ciliogenesis in hTERT-RPE1 cells in cells transiently depleted for *CSPP1* proteins, indicating that CSPP-L is required for cilia formation and/or maintenance (49). Overexpression of *CSPP1* proteins is a driver of aneuploidy caused by *CSPP1*-induced aberrant spindle formation (51). Studies have also shown that CSPP isoforms interact with MyoGEF, a guanin nucleotide exchange factor that localizes to the mid-spindle and cleavage furrow during cell division. MyoGEF and CSPP co-localize on the mid-spindle. The depletion of CSPP with siRNA lead to an interfered localization of MyoGEF at the central spindle, where MyoGEF contributes to the spatiotemporal regulation of cytokinesis (50, 52). Loss of function studies showed that CSPP1 functions in humans affect the primary cilium formation, length and trafficking of ciliary proteins to the axoneme (46). Bi- or multinucleation is not prominent in *CSPP1*-/- cells or reported in *CSPP1*-affected Joubert patients, indicative for that cells can compensate for loss of *CSPP1* during cell division.

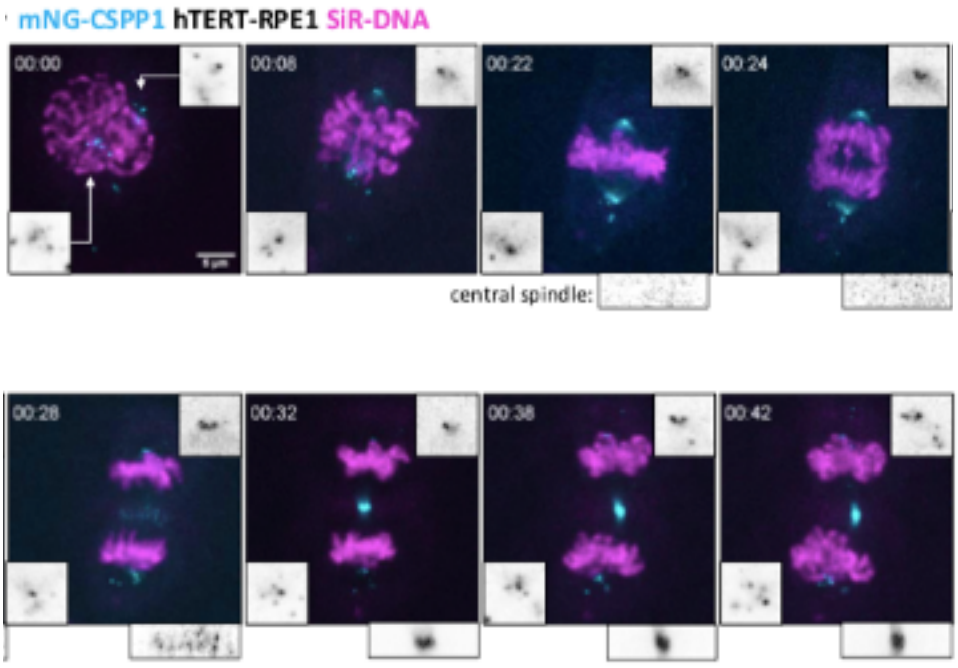

Figure 9: Localization of CSPP-L during mitosis on live cell microscopy. Live cell images were generated by Sebastian Patzke (Department of Radiation Biology, Institute of cancer research (ICR), Oslo University Hospital (OUH)).

1.5 Proximity-dependent biotin identification (BioID)

1.5.1 BioID and miniTurboID

BioID is an enzyme catalyzed proximity labeling method developed to study the interaction of proteins in living cells. It is based on a promiscuous bacterial biotin ligase, BirA*, that efficiently converts supplemented biotin to biotinoyl-5´-AMP, which then reacts with then reacts with surrounding proteins within a 10 nm range. BirA* is fused with a specific protein of interest. When its small molecule substrate biotin is added, endogenous proteins within a 10 nm radius of the promiscuous enzyme will be covalently tagged as biotinylated proteins. Finally, the biotinylated proteins can be purified using streptavidin-coated beads and identified by mass spectrometry (53, 54).
BioID is non-toxic and requires only the addition of biotin to samples to initiate tagging of proteins. A disadvantage of BioID labeling is its slow labeling time, where between 18-24 hours are needed to achieve a sufficient number of biotinylated proteins that can be analyzed. (55, 56).

Therefore new variants of promiscuous biotin ligases with shorter labeling time have been developed. BioID2 and BASU (a biotin ligase enzyme) were first reported. The labeling time was shorter with approximately 16 hours labeling time. TurboID and miniTurbo was introduced thereafter, with drastically shorter labeling time of 10 min or less for miniTurbo (55). miniTurbo have a molecular weight of 28 kD, which is shorter than the BioID and TurboID tag with a molecular weight of 35 kD. (57). TurboID is more active than miniTurbo. The high activity of TurboID makes it possible for the enzyme to use endogenous biotin to biotinylate proteins without addition of exogenous biotin. MiniTurbo is less active and yield therefore less biotinylated proteins without exogenous biotin. Because miniTurbo is smaller in size than TurboID there is a small chance of interference between the fusion protein and miniTurbo or for miniTurbo being in the way of the function of the fusion protein (55, 58). Finally, an alternative proximity ligation technique to BioID is APEX2 (ascorbate perixodase). The advantage of labeling proteins with APEX2 is its short labeling time of 1 minute or less. The disadvantage of using APEX2 is the use of hydrogen peroxide (H_2O_2) which is required when using APEX2 as a labeling enzyme. H_2O_2 is toxic in living samples.

BioID and its variants have been applied on different biological problems, including centrosome and cilia biology. The first-generation BioID versions were extensively used to

explore the interactome of centrosomal and Centriolar satellite proteins by recombinant expression of respective fusion proteins in a human kidney cell line (Hek293) (18, 59) and chicken lymphocyte cell line (DT40) (60).

CSPP1 has hitherto not been tested as bait in any of the studies above, but was identified as prey for several core Centriolar satellite proteins, including PCM1 and CEP131. Given the biological significance of *CSPP1* proteins described above it is thus of high interest to determine its proxymitome by introducing it as bait protein in a relevant cell line system.

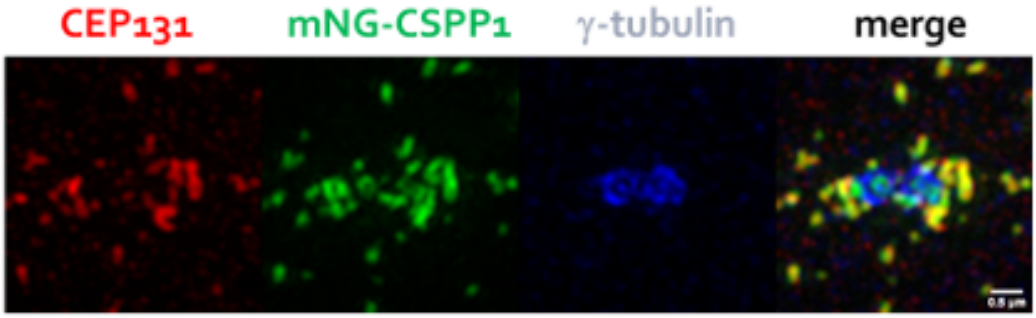

Figure 10: 3D-SIM images by Sebastian Patzke, showing co-localization of mNG-CSPP-L with CEP131 in hTERT-RPE1 cells.

2. Aim of the study

CSPP-L is a protein of the ciliary tip, the axoneme and the basal body in ciliated cells and mitotic spindle microtubules, the mid-body and centrosome during cell division. Microtubule-unbound extra-centriolar CSPP-L localizes to Centriolar satellites. Studies have shown that deleterious mutations in *CSPP1* in humans causes ciliopathies and that overexpression of *CSPP1* proteins, which is found in breast cancer and B cell lymphoma, causes erroneous spindle formation and cell division. While the localization of the CSPP-L protein in cells is well established, its exact function at these localizations is less understood. What is the function of the CSPP-L protein on microtubules? Are the microtubule-associated CSPP-L protein-complexes the same in mitosis and at the cilium? How is localization to and release from the Centriolar satellite compartment regulated? The aim of this project was to generate hTERT-RPE1 cells stably expressing miniTurboID-CSPP-L to enable the determination of the CSPP-L proxymitome at selective sites to gain insights into its molecular function and regulation.

3. Materials and methods

The aim of this study was to generate cells stably expressing the fusion protein miniTurbo-CSPP-L. Two transfer vectors used for lentivirus particle production were generated by LR-reaction of Gateway Cloning. The vectors are different in the length of the linker sequence between the CSPP-L and the miniTurboID sequence. Plasmids were checked for mutations and right insertion of the fusion protein by sanger sequencing before generating the transfer vectors.

LentiX HEK293T cells were used for the lentivirus particle production and hTERT-RPE1 wt cells were transduced with the lentivirus particles. Blasticidin was used to select transfected cells. The expression, localization and biotinylation of the fusion protein were investigated by Western blot, immunofluorescens microscopy and pull-down experiments. Monoclonal cell lines were selected by limited dilution.

3.1 Restriction digestion

The pENTR20-mNG-C1-CSPP-L(50) plasmid was digested with the restriction endonucleases NheI and XhoI to remove the mNG sequence and generate the vector, pENTR20-CSPP-L for Gibson assembly. The New England Biolabs protocol was followed according to the manufacturer's instructions. The digestion solution of total volume 50 µl was made by mixing 5 µl CutSmart buffer (x10) (New England Biolabs), 3 µl pENTR20-mNG-C1-CSPP-L plasmid, 1 µl restrictions enzymes and 40 µl MQH_2O in a 1,5 ml Eppendorf tube (Sarstedt). The sample was incubated for 2 hours at 37°C on a heating block and finally reaction products separated by agarose gel electrophoresis.

3.2 Agarose gel electrophoresis

Agarose gel electrophoresis was applied to separate DNA fragments.
Gels were casted with 1% agarose to resolve the expected fragments of sizes between 731 and 7881 bp. Agarose gels were prepared by weighing 0,5 g agarose (ThermoFisher Scientific) and adding 50 ml of 1x Tris/Acetic Acid/EDTA (TAE) buffer (1,0g/100 ml) (BioRad). The mixture was brought to the boiling point, gently mixed and re-heated until a clear solution was attained. 5 µl of DNA dye SYBRSafe (ThermoFisher Scientific) was added to the clear solution, gently mixed and poured to a gel mold with a well-comb. The gel was hardened for approximately 35-45 minutes. The well-comb was carefully removed, and

the gel was placed in a gel electrophoresis chamber. 1xTAE buffer was poured in the gel electrophoresis chamber, enough to cover the gel. The digestion samples were prepared by adding 10 µl Gel loading dye purple (6x) (Biolabs) to the samples before loading the gel.

The gel was run at 100V for approximately 25 min. The DNA fragments were visualized by using a Chemidoc system with a CCD-camera and a UV light table for excitation of the DNA dye. DNA fragments were extracted from agarose gel by using a Thermo Scientific GeneJet Gel Extraction kit. The kit was used according to the manufacturer's instructions.

3.3 Polymerase chain reaction

The insert fragments, miniTurboID-FLAG(1) and miniTurboID-FLAG(2) were amplified by PCR (Marshall Scientific). These insert fragments were used thereafter, to generate the entry vectors miniTurboID-CSPP-L(1) and (2) by Gibson Assembly. The PCR reaction was optimized to find the optimal annealing temperature and the requirement of dimethyl sulphoxide (DMSO) (Sigma-Aldrich) was tested. An annealing temperature of 52^{o}C and absence of DMSO was found optimal. The Phusion High-Fidelity PCR Kit (ThermoFisher Scientific) was used for the PCR reaction.

A plasmid named pCHD-EF1a-miniTurboID-IRES-Puro (a gift from Elif Firat-Karalar) was used as a template to amplify two miniTurboID-FLAG fragments. The vector was designed for C-terminal fusion of the miniTurboID FLAG tag. Primers were designed to extract the open reading frame of the tag that is framed within an N-terminal start region and a C-terminal linker region, with the effort to create an N-terminal miniTurboID-FLAG-tag that can replace the mNeonGreen-tag in the original pENTR20-mNG-CSPP-L vector construct. The two miniTurboID-FLAG sequences differed by the length of a linker sequence located between miniTurboID and the CSPP1 sequence. The primers used for the PCR reactions are listed below. The primers were designed with overhangs on the 5´and 3´-end, linker sequence and restriction sites for NheI and XhoI.

Primers:

Primers used to generate miniTurboID-FLAG(1)

Primer 1 fwd: 5′-TTTGTACAAAAAAGCAGGCGCTAGCGCTACCGGTCGCCACC**ATGATCCCGCTGCTGAA**- 3′

Primer 2 rev: 5′-TGGAGCGGGAACAGCATGACTCGAGATCTGAGTCCGGTACT**GGATCCCTTGTCGTCATC**- 3′

Primers used to generate miniTurboID-FLAG(2)

Primer 1 fwd: 5′- TTTGTACAAAAAAGCAGGCGCTAGCGCTACCGGTCGCCACC**ATGATCCCGCTGCTGAA**- 3′

Primer 2 rev: 5′- GGCGCGCCGCc**GGATCCCTTGTCGTCATCGTC**- 3′

Primer 3 fwd: 5′- TTTGTACAAAAAAGCAGGCGCTAGCGCTACCGGTCGCCACC**ATGATCCCGCTGCTGAA**- 3′

Primer 4 rev: 5′- TGGAGCGGGAACAGCATGACTCGAGATCTGAGTCCGGTACT**TGGCGCGCCGCCGGA**- 3′

Color coding: Blue: miniTurboID, orange: restriction site, grey: linker sequence and green: CSPP-L

Two PCR reactions were required to generate the insert fragment, miniTurboID-FLAG(2).

Table 1. The PCR sample preparation.

Reagent	Volume (µl)
2x HF buffer	25
Oligonucleotide fwd Primer (5 µmol)	5
Oligonucleotide rev Primer (5 µmol)	5
dsDNA template	2
Nuclease free water	13
Total volume	50

Table 2. PCR program set up.

Cycle step	Temperature	Time	Cycles
Initial denaturation	98°C	30 s	1
Denaturation	98°C	10 s	25
Annealing	52°C	30 s	
Extension	72°C	90 s	
Final extension	72°C	7 min	1
Hold	4°C	-	1

3.4 Gibson assembly

The insert fragments miniTurboID-FLAG(1) and (2) and the linearized mNeonGreen-tag deprived vector pENTR20-CSPP-L were ligated in a ligation reaction called Gibson Assembly to generate entry vectors, pENTR20-miniTurboID-C1-CSPP-L (1) and (2). 10 µl of the NEBuilder HiFi DNA Assembly Master Mix (New England Biolabs) was mixed with 8 µl of the insert fragments and 2 µl of the linearized vector to a total reaction volume of 20 µl in a PCR tube. Samples were vortexed and spun down briefly before incubation for 1 hour at 50°C in a PCR. The samples were stored at -20°C until transformation of *E.coli* Zymo10B (Zymo Research) cells.

3.5 Transformation

Competent *E.coli* Zymo10B cells were transformed with the entry vectors pENTR20-miniTurboID-C1-CSPP-L. The cells and vectors were handled on ice during this reaction. 5 µl of entry vector was transferred to a tube containing 50 µl *E.coli* cells. Each tube was then incubated on ice for 20 minutes followed by heat-shock on 42°C for 60 seconds. The tubes were carefully placed on ice. *E.coli* cells were added 400 µl room-tempered Luria-Bertani (LB) growth medium and transferred to a 1,5 ml Eppendorf tube. Samples were placed on a shaking incubator (Fisher Scientific) for 1 hour at 300 rotations per minutes (rpm) at 37°C. The samples were centrifuged (Hettich) for 2 min at 5000 rpm. Most of the supernatant was removed and the generated pellet containing bacteria cells were resuspended in remaining supernatant (approximately 50 µl solution). The *E.coli* cells were plated on agar plates containing appropriate selection antibiotic (kanamycin or ampicillin) to plasmid. 50 µl bacteria cells were plated on kanamycin (50 µg/ml) agar plate. Agar plates were incubated at 37°C overnight.

Colonies were picked from agar plates and used to inoculate in a 50 ml conical tube containing 5 ml Luria-Bertani (LB) growth medium supplemented with appropriate selection antibiotics (50 µg/ml f.c. for kanamycin or 100 µg/ml f.c. for ampicillin). The conical tubes were incubated overnight in a shaking incubator (Infors HT) at 37°C on 200 rpm to prepare samples for isolation of plasmid.

3.6 Miniprep and midiprep

Miniprep was used to purify the amplified entry vectors. Midiprep was used to amplify concentration of transfer vectors to use for lentivirus particle production. The inoculated samples were used for the midiprep/miniprep. Plasmid DNA was isolated using the NucleoSpin Plasmid Miniprep kit (Macherey-Nagel) and zymoPURE™ Plasmid Midiprep kit (Zymo Research). The kits were used according to the manufacturer´s instructions. The eluted DNA samples were quantified thereafter stored in –20°C. Concentration of eluted DNA was measured by using Nanodrop™ 2000 Spectrophotometer (Thermo Scientific).

3.7 Sanger sequencing

The purified DNA was diluted in sterile water (Aqua B. Braun). A total volume of 10 µl was sent to GATC Biotech for Sanger sequencing. Each tube contained 1 µl plasmid from a miniprep (approximately 500 ng of plasmid) and 5 µl sequencing primer (see section A2 in appendix for sequencing primers) with the final concentration of 5 µM.

3.8 Gateway cloning-LR reaction

The LR-reaction of the gateway cloning was used to generate the transfer vectors for the production of lentivirus particles. The sequenced vectors, pENTR20-miniTurboID-CSPP-L(1) and pENTR20-miniTurboID-CSPP-L(2) were used as the entry vectors for this reaction while the 561-pCDH1-EF1a-GW-IRES-BLAST vector was the destination vector. 1 µl of the entry vector, 1 µl of the destination vector (approximately 250 ng), 6 µl of TE buffer pH8 and 2 µl LR clonase II were mixed in a 1,5 ml Eppendorf tube and incubated for 1 hour at 25°C. The sample was placed on ice after incubation following addition of 1 µl proteinase K. The generated transfer vector was transformed with *E.coli* cells as described in 2.1.5.

3.10 Cell culture

Human Telomerase Reverse Transcriptase immortalized - Retinal Pigment Epithelia 1 (hTERT-RPE1) cells were cultured in Dulbecco´s Modified Eagle Medium: Nutrient mixture F-12 (DMEM/F12) (ThermoFisher Scientific) supplemented with 10% Fetal Bovine Serum (FBS) (ThermoFisher Scientific) and 1% Penicillin/Streptomycin (P/S) (Sigma-Aldrich). Blasticidin was added (diluted 1:1000 from stock solution:10 mg/ml) in cell medium with FBS and P/S for selection of transduced cells. Cells were subcultured using

aseptic technics, when confluency had reached approximately 80%. Cells were then washed once with 10 ml Dulbecco's phosphate buffered saline (PBS) (Sigma-Aldrich) and trypsinated with 1,5 ml trypsin-EDTA (Sigma-Aldrich) solution for about 7 min at 37°C until cells were detached from the cell flask (T75 cell flask, ThermoFisher Scientific) surface. Cells were thereafter re-suspended with 8,5 ml DMEM/F12 supplemented with FBS and P/S. Cells were subcultured in T75 cell culture flasks or T25 cell culture flasks (ThermoFisher Scientific) and incubated at 37°C on 5% CO_2.

The LentiX 293T cell line is a subclone of the transformed human embryonic kidney cells (HEK293T). They are highly transfectable and support high level of viral protein expression. The LentiX 293T cells were used for lentivirus particle production. Cells were handled by the same methods as for hTERT-RPE1 cells. Dulbecco´s Modified Eagle Medium (DMEM) (ThermoFisher Scientific) was used to subculture these cells. LentiX 293T cells are loosely attached to the cell flask surface, detachment of cells was therefore achieved by re-suspension with 10 ml DMEM supplemented with FBS and P/S without an additional step with trypsin.

When seeding cells for experiments, cells were subcultured with the same methods. Cells were counted on a cellcounter *(*Beckman Counter Z2*)* to adjust cell titers when seeding cells for experiment.

3.11 Lentivirus particle production and hTERT-RPE1 transduction

3.11.1 Production of lentivirus particles

A 10 cm^2 dish was coated with 2 ml of a poly-L-lysine (Sigma-Aldrich) solution for 5 min at room temperature. The poly-L-lysine solution was made by mixing 50 ml of sterile water (Aqua B. Braun) in a conical tube with 5 mg poly-L-lysine. Poly-L-lysine solution was removed and the dish was air dryed in a LAF-bench for 2 hours. $5x10^6$ LentiX 293T cells were seeded on the same 10 cm^2 dish with 7 ml DMEM/F12 supplemented with FBS and P/S. Cells were then incubated overnight in a 37°C incubator with 5% CO_2. Transfection of LentiX 293T cells was performed in a BSL-2 virus lab. The transfer vector was mixed with the packaging vectors in a 1,5 ml Eppendorf tube. 15 µg transfer vector was mixed with 15 µg Gag/pol (packaging plasmid), 6 µg Rev (packaging plasmid), 3 µg pVSV-G (envelope plasmid) in 600 µl OPTI-

MEM growth medium (ThermoFisher Scientific). In another 1,5 ml Eppendorf tube, 50 µl lipofectamine 3000 (ThermoFisher Scientific) was mix with 50 µl p3000 (ThermoFisher Scientific) reagent in 600 µl OPTI-MEM growth medium. The solutions with plasmids and lipofectamine were mixed and incubated at room temperature for 25 min. The solution was thereafter drop wise added to the pre-seeded LentiX 293T cells. After the transfection, LentiX 293T cells were incubated overnight at 37°C with 5% CO_2. Cell medium was changed the day after seeding of cells, 10 ml DMEM/F12 cell medium supplemented with FBS and P/S was added to the LentiX 293T cells following incubation for 2 days at 37°C with 5% CO_2. For harvesting of lentivirus particles, a 20 ml syringe (BBRAUN) was used to collect lentivirus particles with a 0,45 µm filter attached to the syringe. Cell medium containing the lentivirus particles was carefully pushed through the filter and into a 50 ml conical tube (Sarstedt). The conical tube containing the lentivirus particles was stored in 4°C until transduction.

3.11.2 Transduction of hTERT-RPE1 wt cells

100 000 hTERT-RPE1 wt cells were seeded in each well of a 6-well plate containing 2 ml DMEM/F12 supplemented with FBS and P/S. hTERT-RPE1 wt cells were incubated at 37°C with 5% CO_2. Lentivirus particles were added to each well, the following day, in different volumes: 500 µl, 200 µl, 100 µl, 50 µl, 10 µl and 0 µl of the virus particle containing supernatant. The transduced cells were further incubated for 2 days. Cell medium was removed from each well and the cells were washed once with 2 ml PBS followed by incubation with 0,5 ml trypsin at 37°C for 5 min. Cells were added 5 ml cell medium with blasticidin (10 µg/ml f.c.) (Invitrogen) in addition supplemented with FBS and P/S. The cell solutions were transferred to T25 cell flasks and incubated in an incubator at 37°C with 5% CO_2. Cell death in each flask was observed.

3.12 Characterization of the established cell lines

SDS-Page and western blot was used to confirm the expression of the fusion proteins in the generated cell lines and to investigate the expression of biotinylated proteins. 100 000 miniTurboID-CSPP-L cells and hTERT-RPE1 wt cells were seeded on 10 cm^2 dishes and incubated at 37°C with 5% CO_2 until desired confluency. For experiments with biotin, cells were added biotin (50 µM f.c. from stock concentration of 50 Mm) (ThermoFisher scientific) after reaching desired confluency and incubated in the timeframes,

5 min, 10 min, 15 min and 30 min. Cells were then lysed or fixed after incubation with biotin.

3.12.1 Lysis

Cell medium was carefully removed, and cells were washed once with 10 ml FBS at room temperature. Cells were placed on ice, PBS aspirated, and then lysed in 750 µl lysis buffer (see section A2 in the appendix for more details). Cell lysates were carefully scraped from the cell dish surface with a cell scraper (Sarstedt) and transferred to a pre-chilled 1,5 ml Eppendorf tube (Fisher Scientifc). Cell lysates were incubated on ice for 15 min and vortexed for 10 sec every 5 min. The samples were centrifuged at 15 000 rpm for 10 min at 4^{o}C. The sample was placed on ice after centrifugation. The supernatant contains proteins while the pellet contains cell debris and insoluble proteins. 50 µl of the supernatant was carefully transferred to a 1,5 ml Eppendorf tube containing 50 µl 2xSLB (Listed in section A2) on ice. The remaining supernatant was used for further experiments. Samples containing 2xSLB were cooked for 5 min at 95^{o}C on, briefly centrifuged and stored in a -20^{o}C freezer.

3.12.2 Purification of biotinylated proteins

High capacity streptavidin agarose resin (ThermoFisher Scientific) was washed with lysis buffer by adding 120 µl agarose resin in a 1,5 ml Eppendorf tube with 1 ml lysis buffer. The sample was centrifuged on 1000 rpm for 1 min at 4^{o}C. Supernatant containing only lysis buffer was removed and 1 ml lysis buffer was added to agarose resin. This step was repeated 2 times. After the last removal of supernatant, 100 µl lysis buffer was added to each tube containing lysates and agarose resin. The remaining cell lysate generated from lysis of cells were used to purify biotinylated proteins. Samples were incubated overnight on rotating wheel at 4^{o}C. Agarose resin with biotinylated proteins assumed attached to them were washed, the samples were centrifuges 2 times on the last washing step to be certain that the supernatant did not contain agarose resin. 50 µl of 2x Sample Loading buffer (SLB) (see section A2 in appendix) was added after removing the supernatant. The samples were briefly vortexed and cooked for 5 min at 95^{o}C. The samples were briefly centrifuged down and stored in a -20^{o}C freezer for separation of proteins on SDS-PAGE.

3.12.3 SDS-PAGE

Sodium dodecyl sulfate polyacrylamide gel electrophoresis (SDS-PAGE) was used to separate proteins by their molecular weight. 15 µl of samples were loaded per well of a 10 well Bio-Rad tgx 4-15% gel. 3 µl of a protein molecular marker (Precision plus protein dual color standards, Biorad) was loaded. Gel was run on running buffer (Tris/Glycine/SDS buffer bought as 10x stock solution from Biorad diluted in 1x MQH_2O) for approximately 30-35 minutes at 200V until lower molecular weight dye marker almost had reached the bottom of the gel.

3.12.4 Western blot

The separated proteins were transferred to
a polyvinylidene fluoride (PVDF) membrane (Biorad) with a trans-blot turbo system from BioRad. Gel was placed in MQH_2O. PVDF membrane was activated in ethanol and then placed in 1x transfer buffer (1L: 200ml 5x trans-blot turbo transfer buffer (Biorad), 600ml MQH_2O, 200ml Ethanol). Whatman papers (Biorad) were placed in 1xtransfer buffer. The transfer sandwich consisted of a stack of Whatman papers, PVDF membrane, gel and a stack of Whatman paper on the top. A roller was used to remove any bubbles. The transfer sandwich was placed in the trans-blot turbo machine (Biorad) for 7 min.

3.12.5 Blocking and incubation with antibodies

The transfer sandwich was disassembled and the PVDF membrane was rinsed in MQH_2O. The PVDF membrane was blocked with (either by 5% w/v fat free dry milk solution in 1x TBST buffer (tris-buffered saline with tween) or 5% Bovine Serum Albumin (BSA) in 1x TBST buffer) for 1 hour. Expression of fusion proteins were detected by incubating with anti-CSPP-L (antibodies are listed in section A3, table 6 and 7 in the appendix) diluted in 5% w/v fat free dry milk overnight at 4°C and for detection of biotinylated proteins samples were incubated with Horseradish Peroxidase (HRP)-streptavidin in 1xTBST buffer at room temperature for 1 hour on rotating bench. HRP conjugated goat-anti-rabbit (GAR) was used as a secondary antibody in 5% w/v fat free dry milk. Samples were incubated for 1 hour on room temperature on rotating bench and then washed 3x5 min in 1x TBST buffer. The PDVF membranes were developed with the ChemiDoc machine
and chemiluminescent Supersignal™ West Dura (Thermo scientific) or supersignal™ PLUS chemiluminescent substrat (Thermo scientific).

3.12.6 Fluorescence microscopy

Fluorescence microscopy was used to investigate the localization of the fusion protein in cells, cilia formation, and expression of biotinylated proteins in the generated cell lines. Coverslips were examined with a 40X objective (NA 1.3) or 63X objective (NA 1.4) objective on a Cell Observer or Zeiss Axiovert microscope system (Carl Zeiss), respectively.

3.12.7 Fixation

70 000 cells were seeded in a 6-well plate containing coverslips and DMEM/F12 supplemented with FBS and P/S. For experiments for cilia formation, cells were serum starved 48 hours prior to fixation. For experiments with biotinylated proteins, cells were added biotin for appropriate timeframe before fixation. Cells were fixated by washing cells once with PBS before adding 2 ml ice cold methanol, covering 6-well plate (ThermoFisher Scientific) with parafilm and storing cells in -20^{o}C for 20 minutes.

3.12.8 Immunofluorescence staining of cells

Cells were stained in a humified chamber made by soaking Whatman paper with MQH_2O, placing the Whatman paper in a box and using a parafilm to cover the Whatman paper. The box was then closed. PBS was added on parafilm dropwise followed by addition of coverslips in PBS with the cell side facing up. Cells were washed with 1 ml PBS, thereafter PBS-AT (1% Bovine serum albumin and 0,5% Triton-X100 in PBS) was added to the coverslips. Cells were blocked with PBS-AT for 15 minutes at room temperature. PBS-AT was removed, and cells were washed once with 1 ml PBS. Cells were then added 25 µl primary antibody diluted in PBS-AT (primary antibodies are listed in the appendix, section A3, table 6). Primary antibody solutions were prepared by dilution with PBS-AT Cells were incubated with primary antibody solutions for 2 hours at room temperature. Cells were washed once with 1 ml PBS following addition of 25 µl secondary antibody diluted in PBS-AT (secondary antibodies are listed in the appendix, section A3, table 7). Cells were incubated with secondary antibody solution for 40 minutes on room temperature. Cells were washed once with 1 ml PBS. Hoechst 33258 (0,6 µg/ml diluted in PBS) (Sigma-Aldrich) was added to each coverslip and incubated for 1 minute at room temperature following washing of cells with 1 ml PBS. The coverslips were rinsed by dipping in MQH_2O and drying coverslips on a paper towel. The coverslips were mounted on microscope slides with the cell side facing

down with ProLong Gold (Invitrogen) as the mounting medium. Cells on coverslips were observed by immunofluorescens microscopy.

3.13 Monoclonal cell line selection

220 000 hTERT-RPE1 miniTurboID-CSPP-L(2) cells were seeded on a petri dish with DMEM/F12 supplemented with FBS and P/S. Cell medium was changed every 3 days until desired colonies had been formed. After generating colonies, six colonies were selected by using sterile paper cloning disc to place over the desired colonies and transferring the paper disc to a 6-well plate containing DMEM/F12. Cell medium was changed every three days until confluence was reached. Cells were expanded by passaged to a T25 cell flask or T75 cell flask.

4. Results

4.1 Construction and cloning of plasmids for lentivirus production

4.1.1 Cloning strategy

The aim of the cloning strategy was the construction of an Entry vector carrying a Gateway cassette that encodes for a miniTurboID-FLAG-CSPP-L fusion protein, which thereafter can be recombined into a Destination vector for lentivirus production. Since we were uncertain about the impact of the linker region on the functionality of the fusion protein, two different linker-constructs were designed. A sequence verified monomeric NeonGreen fluorescent protein (mNG)-CSPP-L cassette bearing Entry vector was available from earlier studies in the lab (50), allowing the replacement of the mNG coding region with miniTurboID-FLAG coding sequences.

The pCHD-EF1a-miniTurboID-IRES-Puro vector (gift from Elif Firat-Karalar), a cloning vector for fusion of the tag to the C-terminus of protein of interest, was used as a template to amplify the miniTurboID-FLAG coding sequence. The PCR fragments were then combined with the mNG-devoid fragment of the pENTR20-mNG-CSPP-L plasmid by Gibson assembly. Assembly products were cloned into *E.coli* Zymo 10B cells, and clones screened by analytical restriction digest of therefrom isolated plasmids to confirm successful ligation. These plasmids were sequenced to verify absence of mutations and that the insert was correctly ligated with the vector before continuing to generate a transfer vector for lentivirus production.

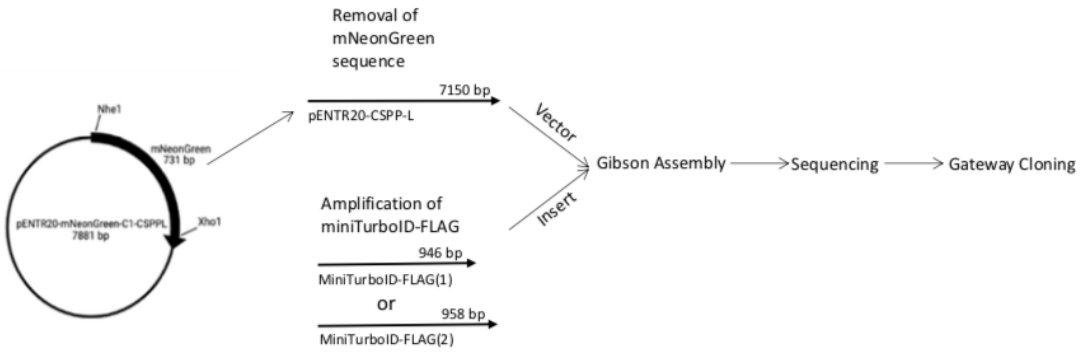

Figure 11: The cloning strategy to generate the transfervectors pENTR20-miniTurboID-CSPP-L(1) and pENTR20-miniTurboID-CSPP-L(2) for lentivirus particle production.

4.1.2 Digestion of plasmid for the removal of mNeonGreen

The pENTR20-mNG-CSPP-L plasmid (figure 4.2) was digested with NheI and XhoI for the removal of the mNeonGreen tag coding sequence. The samples were separated on an agarose gel and screened for the two expected bands with the molecular weight of 7150 bp and 731 bp (figure 4.2B). The smaller band comprises the mNeonGreen coding region. This band was difficult to be visualized on the agarose gel due to its lower intensity. However, the larger band was seen well and had an accurate band size.

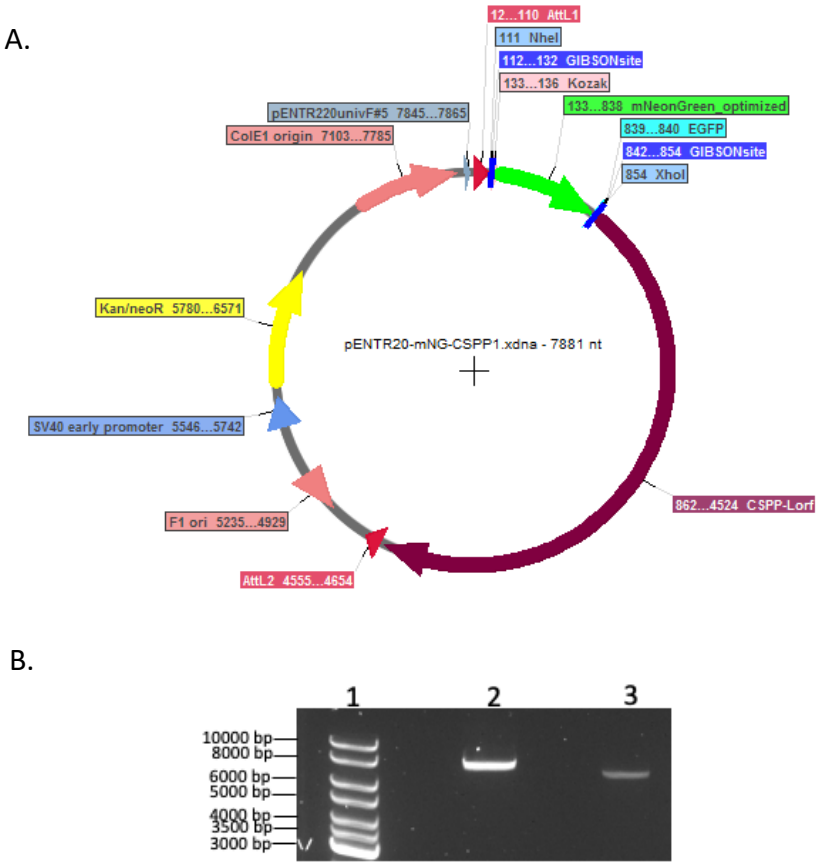

Figure 12: (A) Map of pENTR20-mNG-CSPPL with the restriction sites for the restriction enzymes, NheI and XhoI. (B) Agarose gel electrophoresis of DNA ladder and pENTR20-mNG-CSPPL digested with either NheI alone (lane2, expected band size 7881 bp) or combination of NheI and XhoI (lane3, expected band size of large fragment 7150 bp)

4.1.3 Amplification of the miniTurboID-FLAG sequences

The miniTurboID-FLAG(1) and miniTurboID-FLAG(2) fragments were amplified from the template pCDH-CM-EF1-Puro. In the final construct, the 5´UTR of the mNG-tag on the pENTR20-mNG-CSPP-L (figure 4.2A) plasmid was retained and the mNG-tag replaced with the two respective miniTurboID-FLAG-tag open reading frames with the different linker

regions. Primers used for amplification were designed with pENTR20-mNG-CSPP-L overhangs at 5′and 3′ which were complementary to the ends of the pENTR20-CSPP-L fragments allowing annealing during Gibson assembly. The primers were also designed with linker sequence and re-introduced restriction sites (NheI and XhoI). The extracted miniTurboID-FLAG(1) contained a shorter linker similar to the linker used in the pENTR20-mNG-CSPP-L, construct, while miniTurboID-FLAG(2) had a longer linker (figure 4.3C).

The miniTurboID-FLAG(2) was amplified through two PCR reactions. A reverse adapter primer that introduced a frame-shift and a short linker was used for the first PCR reaction. The amplified sequence was used as a template for the second PCR reaction to amplify miniTurboID-FLAG(2) (figure 3.3A).

PCR products were separated on an agarose gel and the two expected fragments of sizes 946 bp (miniTurboID-FLAG(1)) and 958 bp (miniTurboID-FLAG(2)) were detected (figure 4.3B). These fragments were extracted from the agarose gel, purified and used to generate entry vectors.

A.

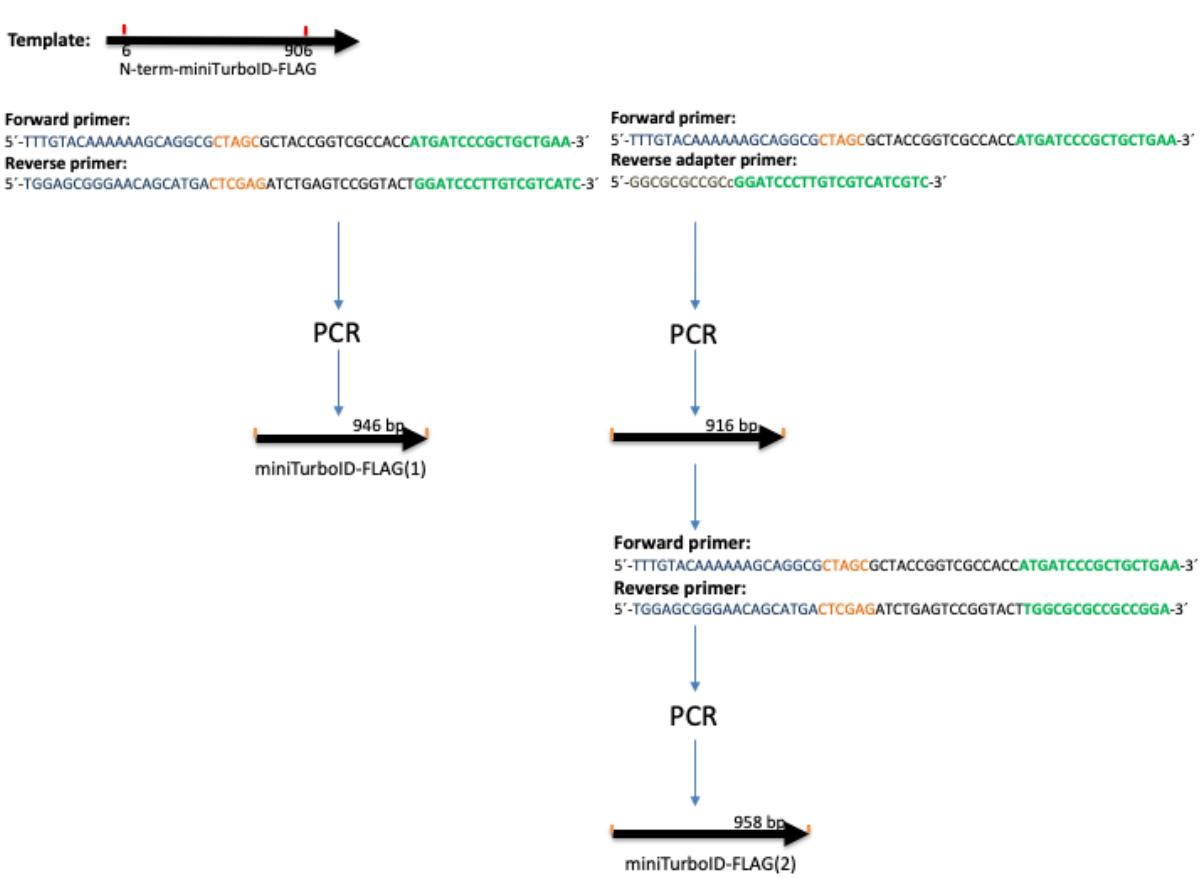

B.

1.

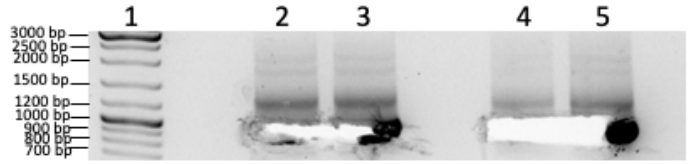

2.

C.

	Blue (BirA), Green (FLAG), Red (linker), Black (CSPP1)
miniTurboID-CSPP-L(1)	..GVIKPWMGGEISLRSAEKPRLQLPPLERLTLDPRASLDDYKDDDDKGSSTGLRSRV**MLFPL**.....
miniTurboID-CSPP-L(2)	..GVIKPWMGGEISLRSAEKPRLQLPPLERLTLDPRASLDDYKDDDDKGSGGAPSTGLRSRV**MLFPL**.....
	Purple (mNG), Red (linker), Black (CSPP1)
mNG-CSPP-L	..RKTELKHSKTELNFKEWQKAFTDVMGMDELYKSGLRSRV**MLFPL**.....

Figure 13: (A) PCR strategies for the amplification of both miniTurboID-FLAG sequences. Blue (pENTR20-mNG-CSPP-L overhangs), Orange (re-introduced restriction sites), Black (linker sequence) and Green (miniTurbo sequence) (B) 1. Figure shows the agarose gel were the PCR products were separated and extracted from. The miniTurboID-FLAG(1) (946 bp) is observed in well

2-3 and the first PCR product (916 bp) before generating miniTurboID-FLAG(2) is shown in well 4-5 in well 4-5. The samples were extracted and purified. Samples in well 4-5 were used as a template in the second PCR reaction 2. Figure shows extracted miniTurboID-FLAG(2) (958 bp) in well 2-3 after the second PCR reaction. (C) Amino acid sequence showing the difference in length of linker in miniTurboID-FLAG(1) and miniTurboID-FLAG(2) compared to linker in mNG-CSPP-L.

4.1.4 Gibson Assembly and sanger sequencing

After amplification of miniTurboID-FLAG(1) and miniTurboID-FLAG(2) the next step was to ligate the inserts with pENTR20-CSPP-L fragments to generate the entry vectors pENTR20-miniTurboID-CSPP-L(1) and pENTR20-miniTurboID-CSPP-L(2). *E.coli* cells were transformed with the entry vectors and plated on Kanamycin containing plates. Five colonies were selected for each construct for further characterization. The plasmids from selected colonies generated with miniTurboID-CSPP-L(1) and miniTurboID-CSPP-L(2) PCR fragments were tested by digestion with Sal1. The three expected fragments with the band sizes, 8076 bp, 4499 bp and 3577 bp were observed on agarose gel (figure 4.4B) which suggested that all selected constructs had inserted the miniTurboID-CSPP-L(1) or miniTurboID-CSPP-L(2) fragments.

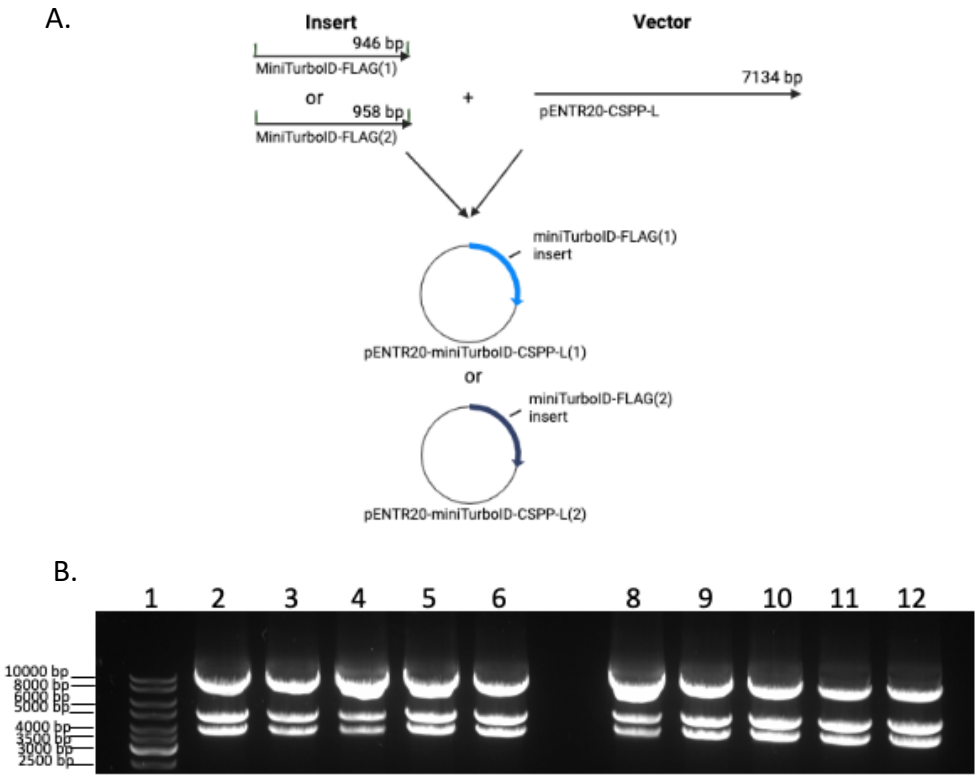

Figure 14: (A) Figure showing miniTurboID-FLAG(1) or miniTurboID-FLAG(2) ligated with pENTR20-CSPP-L and the generated entry vectors pENTR20-miniTurboID-CSPP-L(1) and pENTR20-miniTurboID-CSPP-L(2) (B) The figure present agarose gel with fragments generated after digestion of miniTurboID-CSPP-L(1) and miniTurboID-CSPP-L(2) with Sal1. All three fragments with the expected band sizes 8076 bp, 4499 bp and 3577 bp are shown on gel. Wells 2-6 contain miniprep digests of colonies 1 to 5 of miniTurboID-CSPP-L(1) and wells 8-12 miniprep digests of miniTurboID-CSPP-L(2).

All constructs were Sanger sequenced to check for possible mutations that might have been introduced during PCR (primers see section A1 in appendix). The sequencing results showed one point mutation in two of the constructs (figure 4.5). The 14HA54 (miniTurboID-CSPP-L(1)) and 14HA61 (miniTurboID-CSPP-L(2)) constructs were selected for further cloning.

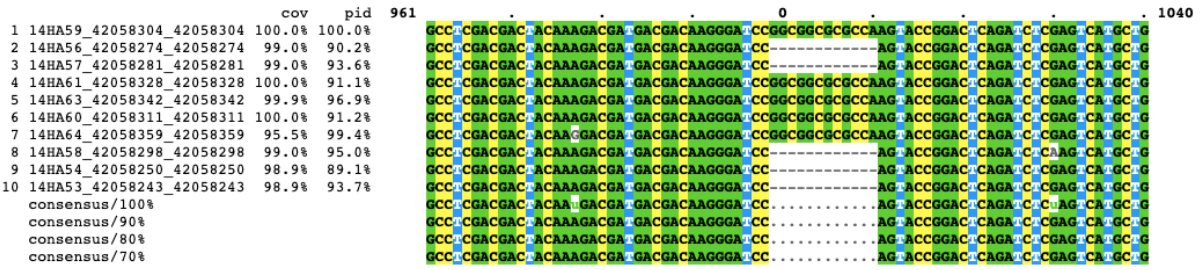

Figure 15: Sequence alignment revealed point mutation in the 14HA64 construct (miniTurboID-CSPP-L(2)) and the 14HA58 construct (miniTurboID-CSPP-L(1)). 14HA59, 14HA61, 14HA63, 14HA60 and 14HA64 is miniTurboID-CSPP-L(2) and 14HA56, 14HA57, 14HA58, 14HA54 and 14HA53 is miniTurboID-CSPP-L(1). The 14HA54 (miniTurboID-CSPP-L(1)) and 14HA61 (miniTurboID-CSPP-L(2)) constructs were selected for further cloning.

4.1.5 Gateway cloning

The final step of the cloning strategy was to generate the transfer vectors, pCDH1-EF1a-BLAST-IRES-miniTurboID-FLAG-CSPP-L(1) and pCDH1-EF1a-BLAST-IRES-miniTurboID-FLAG-CSPP-L(2) for lentivirus production with the LR reaction of the Gateway cloning. *E.coli* Zymo 10B cells were transformed with products of the LR reaction, thereafter the transformed *E.coli* cells were plated on Ampicillin containing plates. Three colonies were selected and expanded. There from isolated plasmids were digested with Sal1 to validate the constructs. The transfer vectors were only confirmed with restriction digestion because gateway cloning is a recombination where no mutation can be introduced. The digested constructs are shown in figure 4.6, one of three constructs (well 3) generated with miniTurboID-CSPP-L(1) had the expected four fragments and all three constructs generated with miniTurboID-CSPP-L(2) had the expected four fragments. Plasmids that were tested in well 3 and 5 were used for lentivirus production.

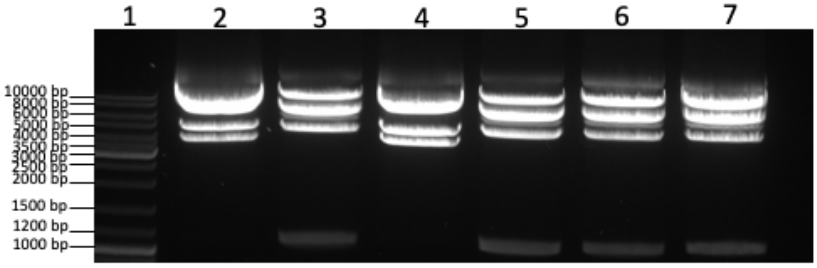

Figure 16: Well 1 contains DNA ladder. The transfer vectors are shown in well 2-4 (pCDH1-EF1a-BLAST-IRES-miniTurboID-FLAG-CSPP-L(1)) and well 5-7 (pCDH1-EF1a-BLAST-IRES-miniTurboID-FLAG-CSPP-L(2)). The transfer vectors in well 3 and 5 had the expected fragment sizes and were further used for lentivirus production.

To summarize, the entry vectors, pENTR20-miniTurboID-CSPP-L(1) and pENTR20-miniTurboID-CSPP-L(2) were successfully generated by Gibson assembly and confirmed by restriction digestion and Sanger sequencing. The sequence validated entry vectors were further used to generate the transfer vectors, pCDH1-EF1a-BLAST-IRES-miniTurboID-FLAG-CSPP-L(1) and pCDH1-EF1a-BLAST-IRES-miniTurboID-FLAG-CSPP-L(2) which were validated by restriction digestion.

4.2 Selection and characterization of cells stably expressing miniTurboID-CSPP-L.

4.2.1 Virus transformation and cell line selection strategy

The Lenti-X 293T cell line is highly transfectable and was used as a packaging cell line for production of virusparticles. Lenti-X 293T cells transfected with transfer vectors and lentiviral vectors were incubated for two days before harvesting lentivirusparticles that were located in the cell medium. The harvested lentivirus was used to infect hTERT-RPE1 wt cells. Different amounts of cell culture supernatant were used for transduction: 500 µl, 200 µl,100 µl, 50 µl or 10 µl was added per well of a 6-well plate pre-seeded with 100.000 hTERT-RPE1 wt cells. Blasticidin was used at 10 µg/ml f.c. to select infected cells. This concentration was determined previously as the lowest concentration that kills all untransduced hTERT-RPE1 wt cells in an experiment (tested concentrations of Blasticidin: 5 µg/ml, 7,5 µg/ml, 10 µg/ml, 15 µg/ml and 20 µg/ml).

Cell death was observed in all wells. Wells containing less transduced cells had the highest amount of cell death, while wells with the majority of transduced cells had the lowest amount of cell death. The highest virus titers had greater amount of cell death than the lowest virus titers. Cells were expanded and passaged four times before being transferred from the virus lab to a cell lab to be sure that there was no lentivirus particle in the cell medium.

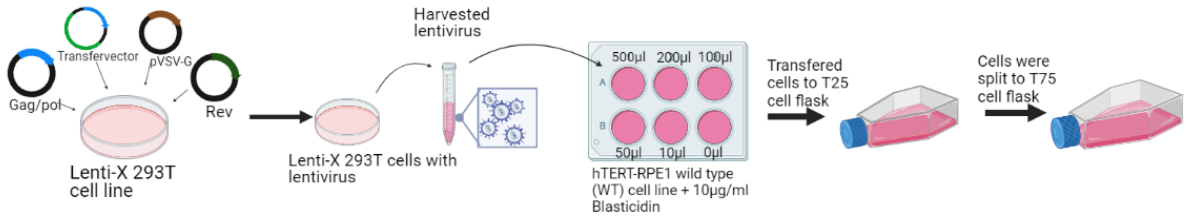

Figure 17: The steps applied to generate cells that stably express miniTurboID-CSPP-L.

4.2.3 Expression of miniTurboID-CSPP-L in the established cell lines

To confirm that the two established cell lines, miniTurboID-CSPP-L(1) and miniTurboID-CSPP-L(2) expressed the fusion protein miniTurboID-CSPP-L, total cell lysates were collected and analyzed on a western blot with an antibody against CSPP-L for detection of both the fusion protein miniTurboID-CSPP-L (175 kDa) and endogenous protein of CSPP-L (150 kDa). The fusion protein is approximately 28 kDa larger than the endogenous protein of CSPP-L.

The fusion protein miniTurboID-CSPP-L and endogenous protein was observed in both cell lines (hTERT-RPE1 miniTurboID-CSPP-L(2) and miniTurboID-CSPP-L(1)) (figure 4.8). Sa,ples of the higher titer were ran on a separate gel then protein samples obtained from the lower titers. Untransduced hTERT-RPE1 wt cells were used as the control cell line.

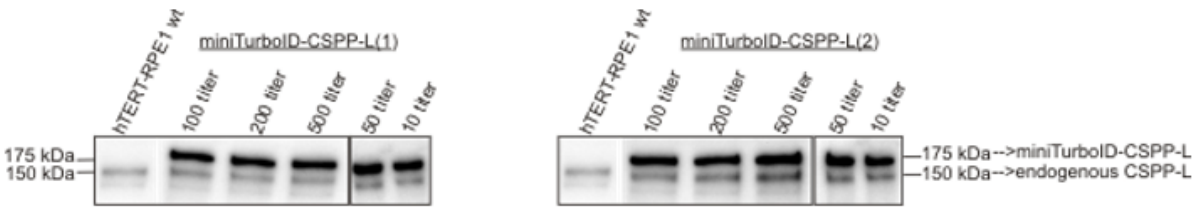

Figure 18: Detection of the fusion protein miniTurboID-CSPP-L and the endogenous protein of CSPP-L in the generated cell lines. The fusion protein was detected in all cell lines miniTurboID-CSPP-L(1) and miniTurboID-CSPP-L(2). MiniTurboID-CSPP-L and endogenous CSPP-L was detected with the CSPP-L antibody.

For both constructs the miniTurboID-CSPP-L cells of the 10 µl titers were selected for further experiments.

4.2.4 Co-localization of miniTurboID-CSPP-L with the Centriolar satellite protein CEP131.

After confirming the expression of the fusion protein in the cell lines, the next step was to observe its subcellular localization and to confirm its co-localization with CEP131 by fluorescens microscopy. To this, cells were fixed and stained with an antibody against the FLAG protein for detection of fusion protein and an antibody specific to CEP131.
The images of selected regions displayed in figure A show co-localization of the fusion protein (red) and CEP131 protein (green) in both cell lines.

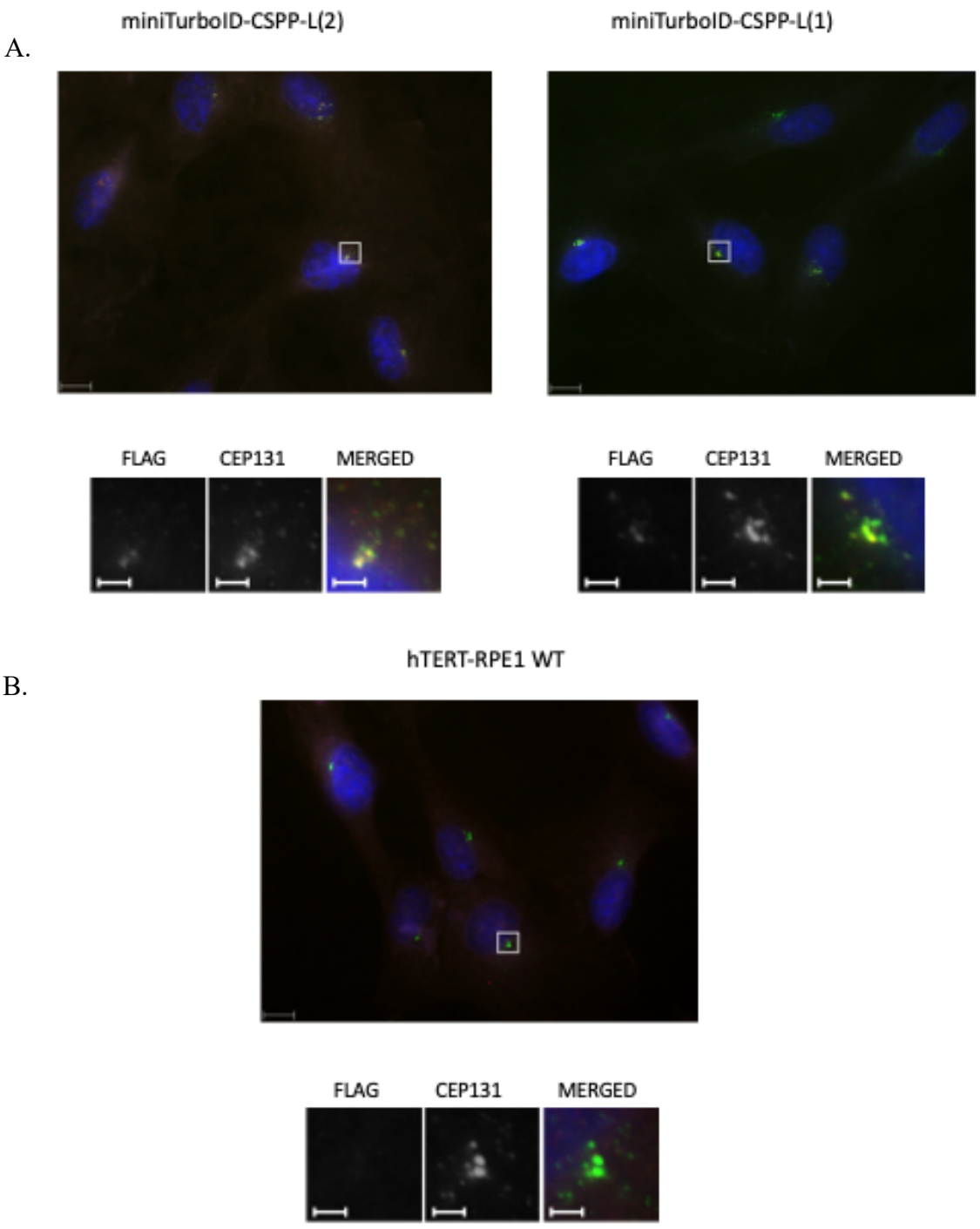

Figure 19: Co-localization of the fusion protein with CEP131.Transduced (A) and untransduced (B) cells stained with antibody against the FLAG (red) protein, antibody against CEP131 (green) and DAPI (staining of DNA) (blue). The miniTurboID-CSPP-L cells of 10 µl titer (A) were used for this experiment and untransduced hTERT-RPE1 wt cells were used as the control cell line (B). The scale bar is 10 µm for the images of the whole field and 2 µm for the images of the selected regions.

After observing the fusion protein in the cell lines and validating the co-localization of the fusion protein with the CEP131 protein, the next step was to test the biotinylation-activity of the BirA*-FLAG-CSPP-L protein. The expression level of the fusion protein varied between cells, some cells had higher expression level while other cells had lower expression level of the fusion protein. The localization pattern of the fusion protein was approximately the same, the fusion protein localized to the satellites and centrosome. Cells of higher titers were frozen and preserved in liquid nitrogen.

4.2.5 Biotinylation assay

To test for the biotinylation-activity of the introduced miniTurboID-CSPP-L constructs biotin was added to cells at 50 µM final concentration and cells incubated for different durations prior to fixation and detection of biotinylated proteins by fluorescence-labeled streptavidin. Cells were incubated with biotin for 30 min, 15 min, 10 min and 5 min. The biotinylation was followed by fixation and staining of cells with antibody against the FLAG protein, CEP131 antibody, DAPI for staining DNA and Fluorescein Isothiocyanate (FITC)-streptavidin for staining the biotinylated proteins. hTERT-RPE1 wt cells were used as a control cell line and were stained with the same antibodies. The goal with the biotinylation assay was to validate that the miniTurboID-CSPP-L protein biotinylates proteins, investigate the localization of the biotinylated proteins and determine the optimal duration for the biotinylation with minimal background biotinylation.

Figure 4.10 show the results of the biotinylation assay with miniTurboID-CSPP-L(1) (A), miniTurboID-CSPP-L(2) (B) and hTERT-RPE1 wt cells (C). The cell lines were supplemented with biotin for different durations to determine the optimal time for BirA* protein to biotinylate neighboring proteins. Cells were stained with antibody against the FLAG protein (white), antibody against CEP131 protein (red), FITC-streptavidin to detect biotinylated proteins (green) and DAPI to detect DNA (blue).
The results of the biotinylation assay revealed the co-localization of the biotinylated proteins with the fusion protein and the CEP131 protein. The background biotinylation was low and homogenous, but varied between different time frames. This may rather reflect a staining procedure variation then a biological variation. Images of selected regions revealed low but detectable biotinylated proteins even after 5 min, which is in line with the short labeling time expected from the miniTurboID system.

A.

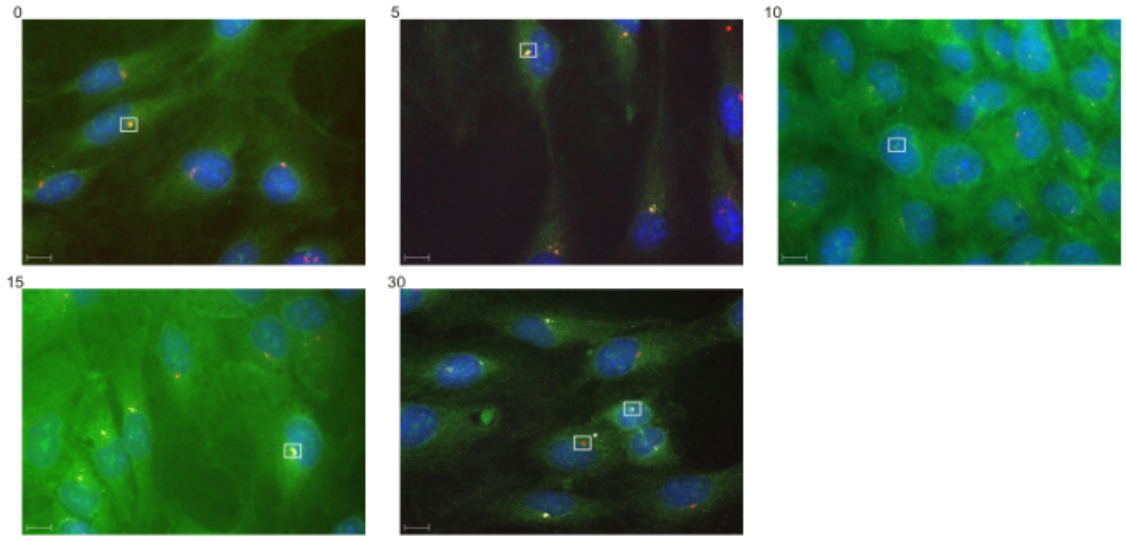
0
5
10
15
30

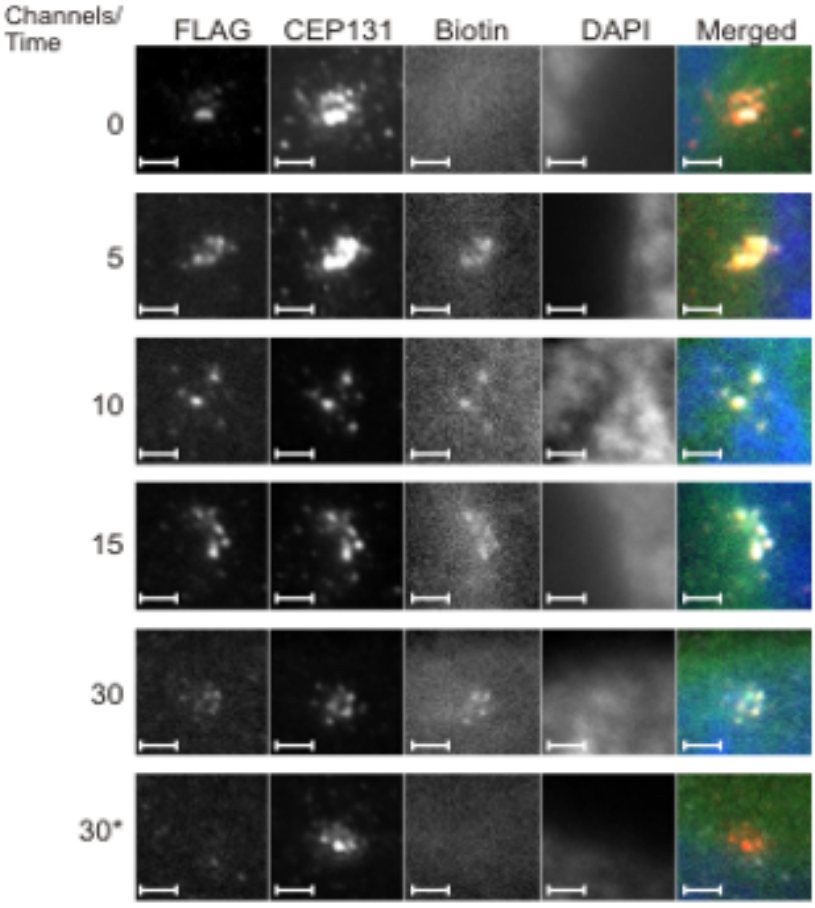
Channels/
Time
FLAG
CEP131
Biotin
DAPI
Merged
0
5
10
15
30
30*

B.

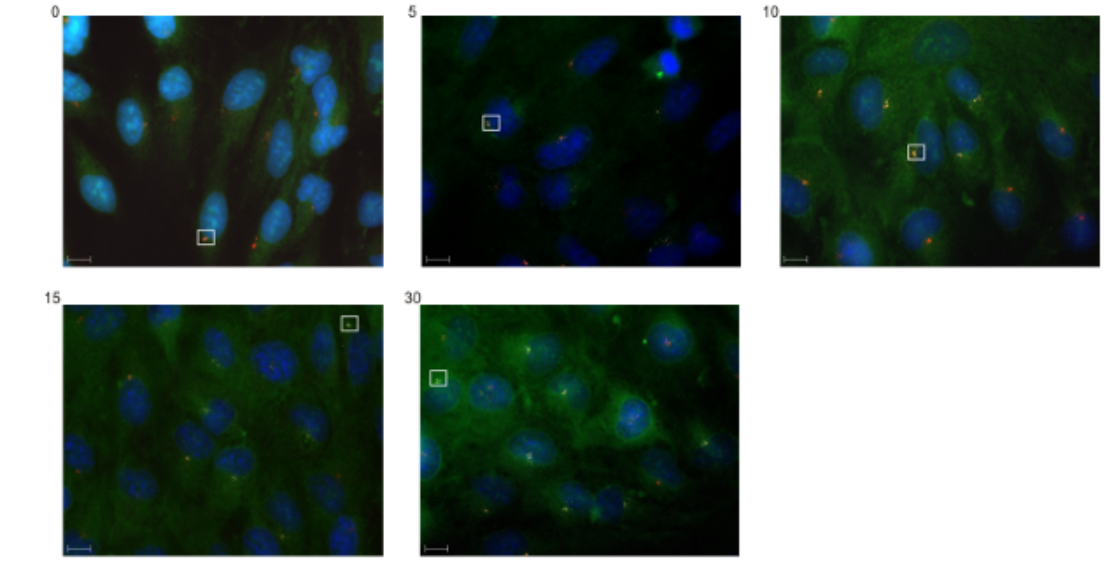
0
5
10
15
30

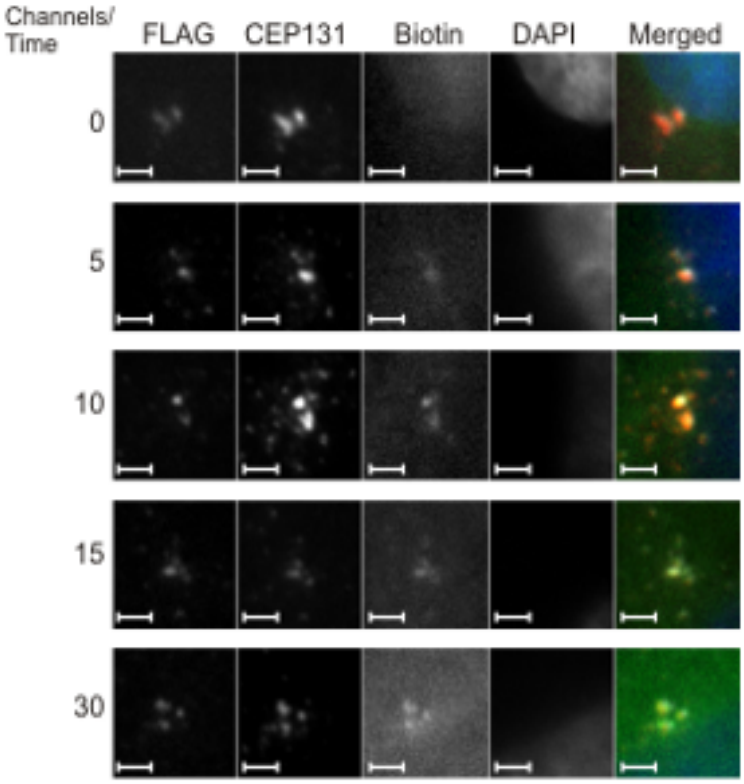
Channels/
Time
FLAG
CEP131
Biotin
DAPI
Merged
0
5
10
15
30

C.

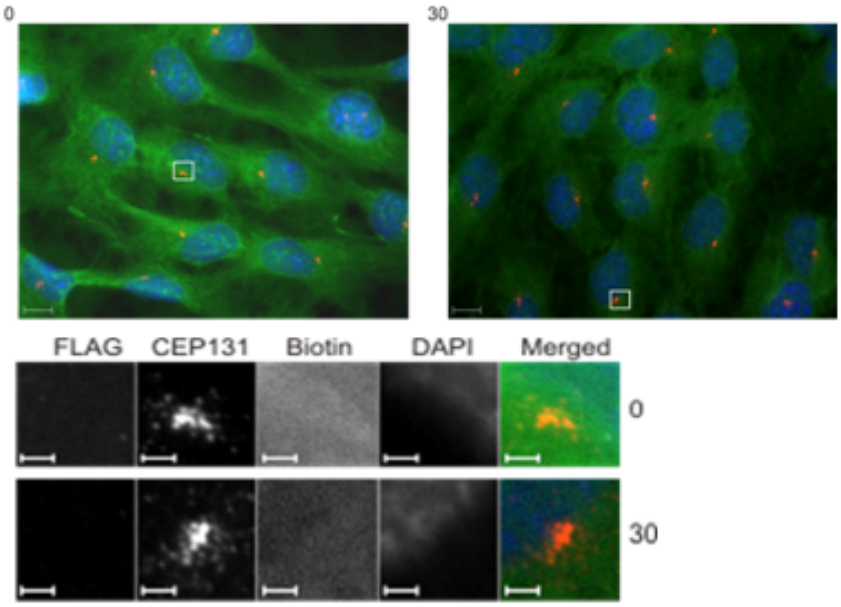

Figure 20: Biotinylation activity of miniTurboID-CSPP-L(1) and miniTurboID-CSPP-L(2) in different timeframes. miniTurboID-CSPP-L(1) (A) and miniTurboID-CSPP-L(2) (B) cells were added biotin in 5 min, 10 min, 15 min and 30 min. hTERT-RPE1 wt cells (C) is the control cell line and was also added biotin for 30 min. The untreated control cells (0) were not supplemented with biotin. Selected region marked with, 30*, show staining of a cell which did not express the fusion protein. Cells were stained with antibody against the FLAG protein (white) for detection of the fusion protein, antibody against CEP131 (red), FITC-streptavidin (green) for detection of biotinylated proteins and DAPI (blue) for detection of DNA. The scale bar for the images of the whole field is 10 μm and 2 μm for the selected regions.

4.2.6 Localization of the fusion protein in mitosis

The fusion protein was also tested for its localization pattern during stages of mitosis. The CSPP-L protein is known to localizes on the centrosomes in prophase, the mitotic spindle and centrosomes during metaphase, the mid-spindle in anaphase and on the mid-body in telophase and cytokinesis (figure 9). A monoclonal cell line (subclone1) were used for this experiment. Cells were stained with antibody against the FLAG protein to detect the fusion protein, anti-EB3 to detect MTOC and the plus-end of the microtubules, FITC-streptavidin to detect biotinylated proteins and DAPI for detection of DNA.

The low staining of the fusion protein in mitosis can be caused by the affinity of the antibody used for detection of the fusion protein. Detection of biotinylated proteins on the same images indirectly indicates localization of the fusion protein.

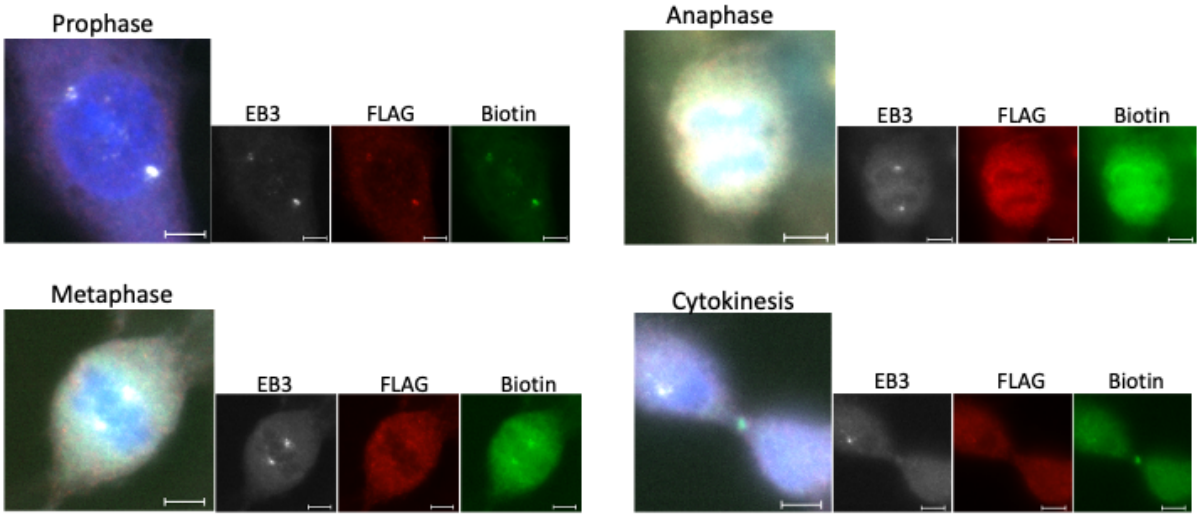

Figure 21: Figure display localization of fusion protein in miniTurboID-CSPP-L cells during mitosis on fluorescence microscopy. Cells were stained with anti-EB3 (white) to detect the MTOC, antibody against the FLAG protein (red) to detect the fusion protein, FITC-streptavidin (green) to detect biotinylated proteins and DAPI (blue) for detection of DNA. miniTurboID-CSPP-L cells were treated with biotin for 10 minutes. The scale bar on the images is 10 μm.

4.2.7 Purified biotinylated proteins

The immunofluorescence based biotinylation assay confirmed site-specific biotinylation by the two different miniTurboID-CSPP-L fusion proteins. Next, an analytical-scale pulldown experiment was performed to purify biotinylated proteins from total cell lysates. miniTurboID-CSPP-L(1) cells and miniTurboID-CSPP-L(2) cells were added biotin in the same timeframes as in the biotinylation assay (figure 4.10). Cell lysates from 100 000 cells were collected and biotinylated proteins were extracted with high-capacity streptavidin agarose resin. The extracted biotinylated proteins were detected on western blot with Horseradish Peroxidase (HRP)-Streptavidin. Only a low signal was observed, we speculated that the low enrichment of biotinylated proteins may have been caused by the heterogeneity of fusion protein expression between cells in the polyclonal population, whereof a larger fraction depicted very low expression. This was resolved by selecting monoclonal cell lines. The miniTurboID-CSPP-L(2) cells of the lower titer (10 μl) had a higher fraction of cells expressing the fusion protein at modest levels and was therefore used to generate a monoclonal cell line to attain uniform expressing cells. Figure 4.11 show extracted biotinylated proteins from a monoclonal cell line (subclone1) after incubation with biotin for 30 minutes. hTERT-RPE1 wt cells were used as a control cell line.

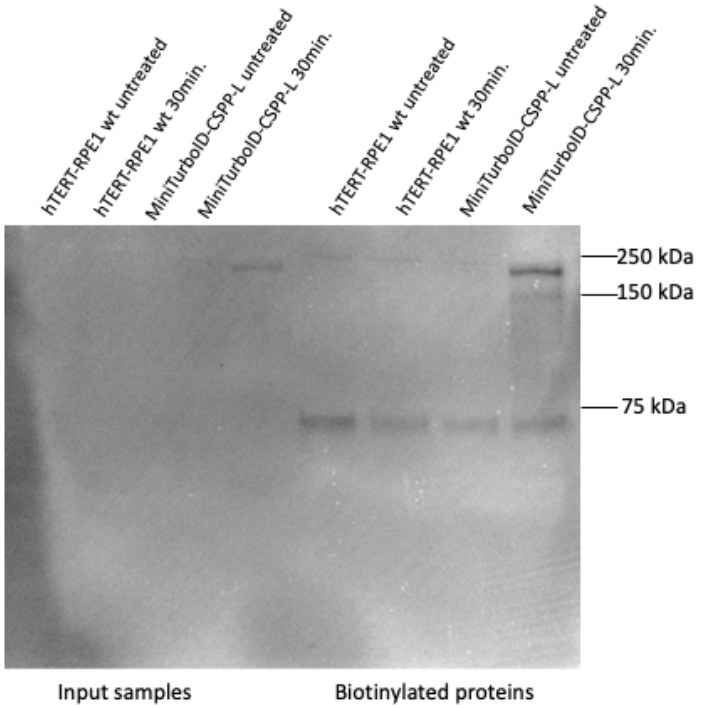

Figure 22: Figure show western blot results of purified biotinylated proteins of miniTurboID-CSPP-L cells and hTERT-RPE1 wt cells (control cell line) treated with biotin in 30 minutes. high-capacity streptavidin agarose resin was used to extract biotinylated proteins. Proteins were stained with HRP-streptavidin for detection of biotinylated proteins. Treated and untreated cells were used for this experiment.

4.3 Selection and characterization of monoclonal cell lines

The lowest titer of the miniTurboID-CSPP-L(2) cell line was selected to isolate a monoclonal cell populations. The hTERT-RPE1 miniTurboID-CSPP-L(2) cell batch contained the highest frequency of cells expressing the fusion protein and was therefore selected to generate a monoclonal cell line. Approximately 220.000 cells were seeded on a 150 mm petri dish to generate well-separated colonies that are formed from single cells. Six colonies were then selected and transferred to a 6 well-plate with cell medium by using a sterile cloning disc. Cells were further expanded and passaged.

The generated monoclonal cell lines (referred to as subclone1, subclone2, subclone3 and subclone4) were observed with a fluorescens microscope and analyzed on western blot to evaluate the expression levels of the fusion protein miniTurboID-FLAG-CSPP-L and endogenous protein of CSPP-L. One of the four cell lines (subclone1) was then selected for

further studies of cilia formation and to validate the co-localization of the fusion protein with the satellite protein CEP131.

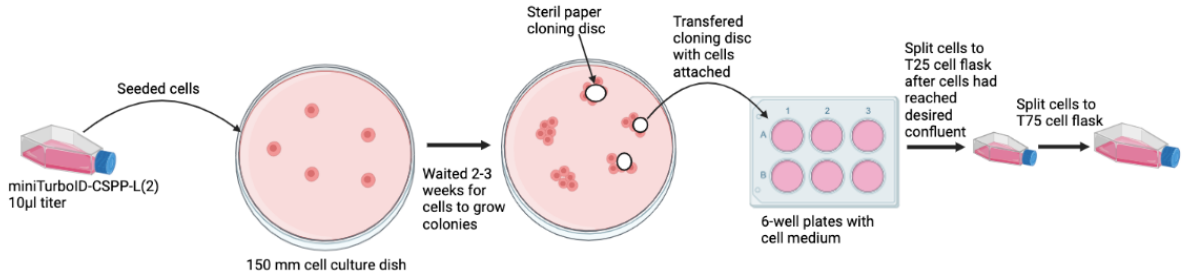

Figure 23: Strategy for the selection of monoclonal cell lines

4.3.1 Characterization of the monoclonal hTERT-RPE1 miniTurboID-CSPP-L cell line by fluorescence microscopy and western blot analysis

The four selected subclones were examined for expression and subcellular localization of the fusion protein. Observation of the subclones on immunofluorescence microscopy confirmed a uniform expression of the fusion protein (figure 4.13) in all cells of the four respective subclones. This suggested a successful isolation of single subclones from the heterogenous parental population. The fusion protein localized to small granules reminiscent of the Centriolar satellites.

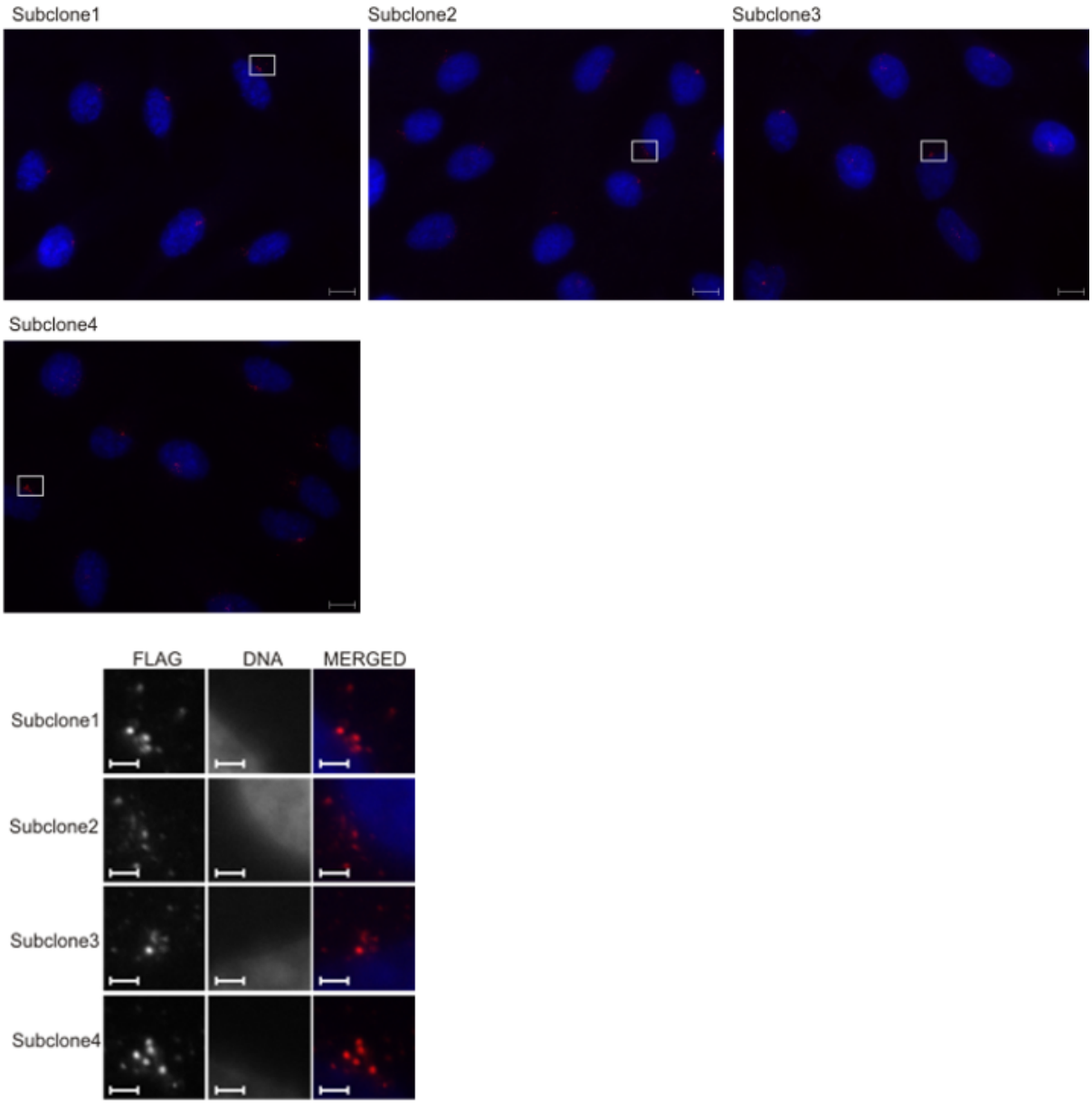

Figure 24: Fluorescens microscopy images of all four monoclonal cell lines. Cells were fixed with methanol and then stained with the antibody against the FLAG protein (red) and Hoechst (DNA) (blue). The images revealed a monoclonal cell population in all cell lines. The scale bar is 10 μm for figures of the whole fields and 2 μm for the selected regions.

4.3.2 Co-localization of the fusion protein with CEP131

The co-localization of the fusion protein with CEP131 was validated with cells in subclone 1. The cells were fixed and stained with the antibody against the FLAG protein and the CEP131 antibody and then examined by fluorescens microscopy. The results confirmed the co-localization of the fusion protein and the CEP131 protein (figure 4.15). Non-transduced parental hTERT-RPE1 wt cells were used as the control cell line.

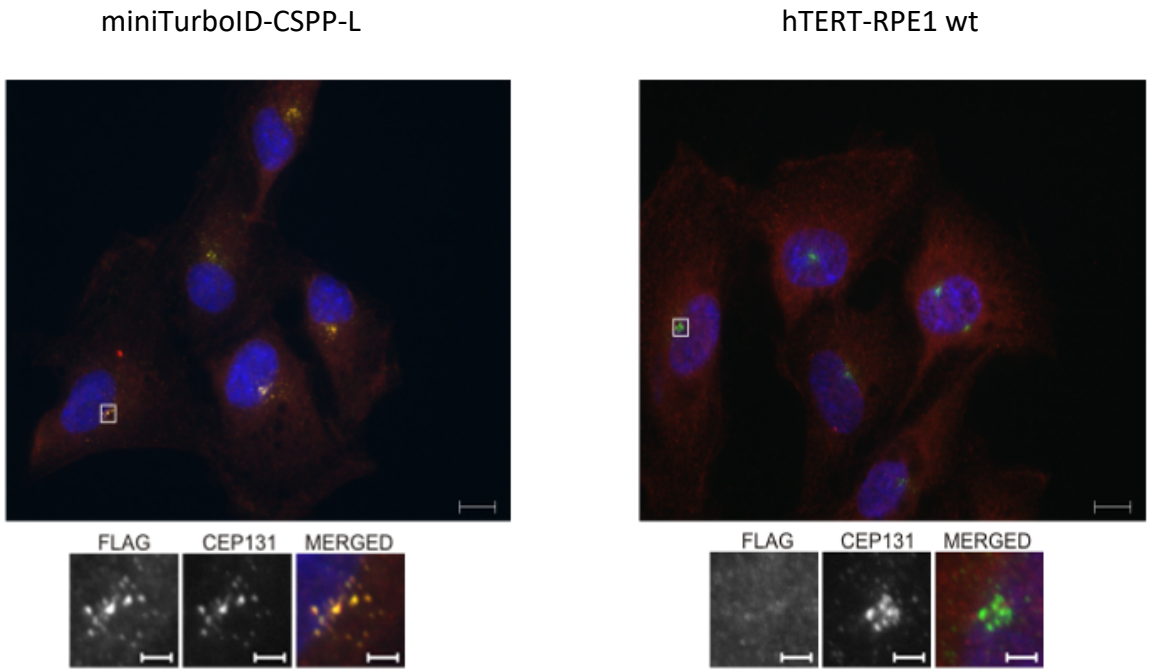

Figure 25: Fluorescens microscopy analysis of miniTurboID-CSPP-L cells stained with CEP131 antibody (green) and antibody against the FLAG protein (red). hTERT-RPE1 wt cells were used as the control cell line.

4.3.3 Expression level of the fusion protein in the subclones

The cell lines were also analyzed on western blot to evaluate the expression level of the fusion protein miniTurboID-CSPP-L (175 kDa) and the endogenous protein CSPP-L (150 kDa). Cell lysates were collected and analyzed by western blot. The antibody against CSPP-L was used to simultaneously detect the fusion protein and the endogenous protein.

The fusion protein was observed in all cell lines (Figure 4.14) ang higher than the expression of the endogenous protein (decreasing from subclone 1 to subclone 4).

Band intensities were quantified to estimate the degree of over-expressed fusion protein in respect to the endogenous protein. Densitometry was done with ImageLab Software, where the expression of the fusion protein in all four monoclonal cell lines was analyzed against the level of endogenous CSPP-L protein in the same cell lines. The subclone3 had the highest expression of the fusion protein, showing 6x higher expression compared to the endogenous protein. The remaining monoclonal cell lines had approximately 5x higher expression of the fusion protein. There was no loading control used in this experiment because of the assumptions that the endogenous protein of CSPP-L is expressed in all cells at the approximately same level. The experiment was done once, therefore these results only show an estimate expression of the fusion protein in the monoclonal cell lines.

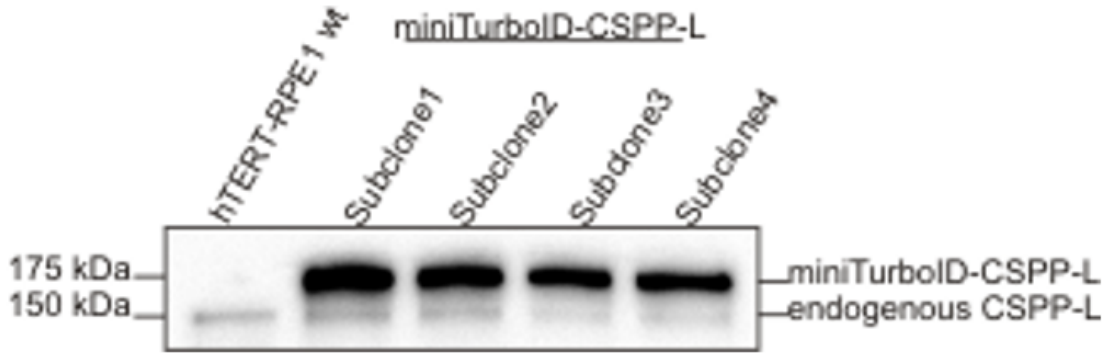

Figure 26: Western blot analysis of the monoclonal cell lines expressing miniTurboID-CSPP-L. Cell lysates were collected and analyzed on western blot. The CSPP-L antibody was added to detect both the fusion protein miniTurboID-CSPP-L and the endogenous protein CSPP-L. hTERT-RPE1 wt cells were used as the control cell line.

4.3.4 Cilia frequency

The monoclonal cell lines were investigated next for their capacity of cilia formation and the subcellular localization of miniTurboID-CSPP-L in ciliated cells. Cells were serum starved for 48 hours to induce cilia formation, and then fixed and stained with the antibody against the FLAG-tag and ARL13B, a small GTPase specifically localized to the primary cilium. Cilia formation in the monoclonal cell lines varied and only a minority of the cells were able to form cilia. The highest frequency of the ciliated cells were observed in subclone1 (hereafter referred to as miniTurboID-CSPP-L). miniTurboID-CSPP-L cells were therefore selected for further studies of cilia formation.

The formation of cells in miniTurboID-CSPP-L cells was observed by fluorescens microscopy (figure 4.15A). hTERT-RPE1 wt cells were used as the control cell line. Cilia frequency in miniTurboID-CSPP-L cells were compared to cells from the control cell line. Cilia frequency in miniTurboID-CSPP-L cells were 42% versus 72% in hTERT-RPE1 wt cells (Table 3). The frequency of unciliated cells was 59% for miniTurboID-CSPP-L cells and 28% for hTERT-RPE1 wt cells. Collectively, these results indicate that the four selected subclones have difficulties forming cilia, compared to hTERT-RPE1 wt cells. Alternatively, this specific clone may have acquired fusion-protein expression unrelated modifications that impede cilia formation. The results are based on two experiments and should be repeated to allow statistical assessment.

A.

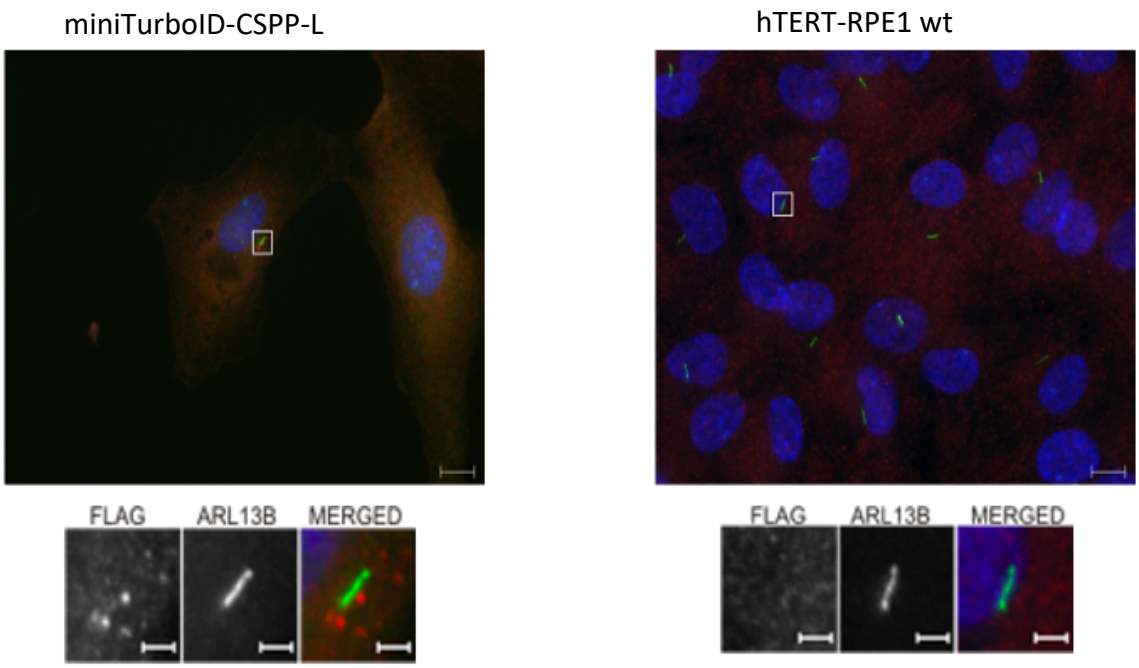

B.

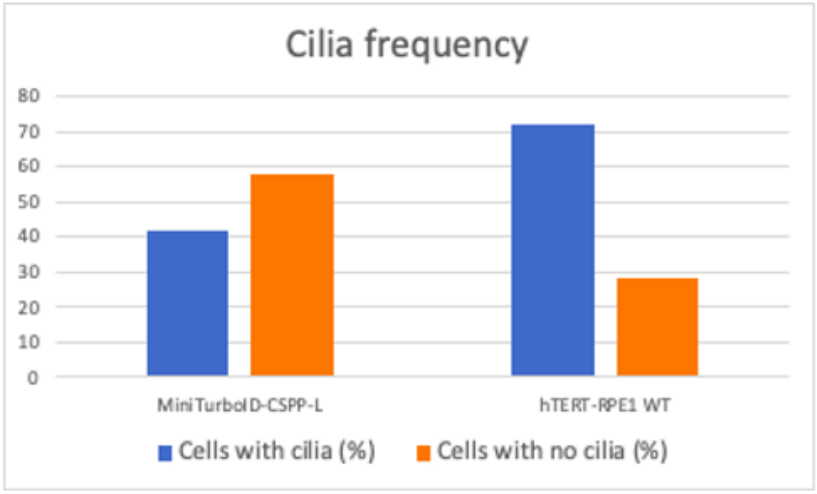

Figure 27: Immunofluorescence microscopy images of cilia formation and cilia frequency 48 hours post serum starvation. (A) figures show miniTurboID-CSPP-L cells and hTERT-RPE1 wt cells (control cell lines) stained with ARL13B antibody (green) and antibody against the FLAG protein (red). (B) Cilia frequency for miniTurboID-CSPP-L and hTERT-RPE1 wt cells. The values correlate from two experiments. 600 cells of miniTurboID-CSPP-L and 600 cells of hTERT-RPE1 wt were used for the experiments.

Table 3: Cilia frequency in miniTurboID-CSPP-L cells and hTERT-RPE1 wt cells. The results are average of two experiments.

	Cells with cilia (%) / *mean (M) value of each experiment*	Cells with no cilia (%) / *mean (M) value of each experiment*
MiniTurboID-CSPP-L	42 % / *M= 45, 39*	59 % / *M= 54, 61*
hTERT-RPE1 WT	72 % / *M= 79, 64*	28 % / *M= 21, 34*

The localization of the fusion protein on ciliated cells was also investigated. Previous studies have located the CSPP-L protein on the transition zone, cilia axoneme and on the tip of the cilia (46) therefore the fusion protein was examined for the same localization on cilia. The miniTurboID-CSPP-L cells were serum starved for 48 hours and stained with the antibody against the FLAG protein and the ARL13B antibody. The fusion protein was observed on the centriolar satellites around the cilia but not on the cilia axoneme or the tip of the cilia. The localization of the fusion protein in ciliated cells needs to be further studied.

To summarize, four monoclonal cell lines were generated from the miniTurboID-CSPP-L(2) hTERT-RPE1 batch that was transduced with10 µl of virus suspension cells. The generated cell lines were confirmed on western blot for expressing both the fusion protein and endogenous protein and was also observed in fluorescens microscopy. One of four monoclonal cell lines, miniTurboID-CSPP-L was selected for further studies of cilia formation and co-localization of the fusion protein with CEP131.

5. Discussion

The main purpose of this project was to generate hTERT-RPE1 cells stably expressing miniTurboID-FLAG-CSPP-L and to test its biotinylation capacity. Such cell line would enable the determination of localization-specific proxymitomes of CSPP-L and thus provide valuable insides into its regulation, if the fusion protein resembles the localization pattern of the endogenous protein.

5.1 Generating hTERT-RPE1 miniTurboID-CSPP-L cell lines

The cell lines were generated by transfecting hTERT-RPE1 cells with lentiviral particles generated in Lenti-X HEK293T cells with transfer vectors, packaging vectors and envelope vectors. Two transfer vectors were generated, dissimilar in the length of the linker sequence. The transfer vectors were generated by restriction digestion, PCR amplification, Gibson assembly, Gateway cloning and sequence verified. The restriction digestion of pENTR20-mNG-CSPP-L vector was achieved by the endonucleases, NheI and XhoI. A shorter DNA fragment of the mNG-sequence was not seen on agarose gel, but the larger DNA fragment of the mNG-devoid vector with the expected molecular weight was observed after separation on agarose gel (figure 3.2A). The DNA fragment with the molecular weight corresponding to the mNG devoid vector was extracted despite not being able to visualize the short DNA fragment corresponding with the mNG-sequence. The shorter fragment migrated faster during separation on gel making it difficult to visualize. The reason for this was the lower molecular weight of the DNA fragment making it difficult for it to be taken up by the fluorescent dye, SybrSafe in the gel. SybrSafe migrate also in opposite direction than the DNA migrate during electrophoresis. This means that the bottom of the gel contains a lower concentration of the SybrSafe. This effect of SybrSafe in the gel can be prevented by adding SybrSafe in the loading buffer.

The generated entry vectors and transfer vectors were transformed into *E.coli* Zymo10B cells. Colonies were picked and inoculated to purify enough DNA plasmids for further experiments. The purified DNA plasmids were digested and separated on agarose gel to check for expected DNA fragments after digestion.
Colonies for virusparticle production were chosen based on the digestion pattern. If multiple clones were correct then one clone was randomly picked.

hTERT-RPE1 cells were transfected with different amounts of lentivirus (500 µl, 200 µl, 100 µl, 50 µl and 10 µl of virusparticle comprising cell culture supernatant). A polyclonal cell population is created because of the multiple integration events for the lentivirus to be integrated in the genome. Cells were transfected with lentivirus particles and incubated in growth medium containing a selection antibiotic called Blasticidin. The transfer vectors were generated with an antibiotic resistance gene called Blasticidin, addition of the antibiotic made it possible for selecting transfected cells. The antibiotic concentration of 10 µg/ml was chosen based on a dose-response experiment that tested for the minimal concentration needed to kill all cells in the course of one week. A cell is stably transfected when lentivirus is integrated into the genome and becomes an inherited part of it. Thereafter, the integrated gene of interest will be replicated and expressed by the genome.

The selection antibiotic in the growth medium selected for transfected cells. Non-transfected cells would die, because they lack the antibiotic resistance gene for Blasticidin. The blasticidine-resistance conferring gene is encoded on the same mRNA as the fusion-protein (bi-cistronic mRNA). Its translation is driven by an internal ribosomal entry site (IRES), but its expression is coupled with the fusion protein, by being controlled by the same promoter element (EF1a promoter in our case). A polyclonal cell population also means that expression level of the fusion protein varies in between cells. Cells transfected with high concentration of lentivirus particles showed generally a lower degree of cell death, while cells transfected with low concentration of lentivirus particles had higher amount of cell death. Cells in lower titers were expected to have lower level of expression because of low of the low integration events. Cells were sub-cultured in growth medium containing Blasticidin with a stabile concentration of 7,5 µg/ml to maintain a pool of stable expressing cells. Despite the antibiotic selection and coupled expression of fusion protein and resistance-conferring protein many cells in the higher virus titer transductions stopped expressing the fusion protein. The same behavior was observed in cells of the lower titers but to lower degree. This may be indicative for a counter selection, i.e. cell do not tolerate higher level expression of the fusion protein. The generated cell lines were dissimilar by the length of the linker sequence. miniTurboID-CSPP-L(1) contained a similar length of linker sequence as in the pENTR20-mNG-CSPP-L vector and the miniTurboID-CSPP-L(2) contained a longer linker sequence (figure 3.3C). We did not observe any differences in terms of expression or localization pattern of the fusion proteins in the transduced cell lines. It was decided to

generate monoclonal cell lines by using the miniTurboID-CSPP-L(2) cells from the lower titer.

To obtain uniform cell lines, monoclonal cell lines were generated by dilution. miniTurboID-CSPP-L(2) cells of 10 µl titer were used to generate monoclonal cell lines, because the cell line contained more cells expressing the fusion protein when observing the cells in fluorescence microscopy. Six colonies were picked and expanded. Four out of six colonies contained a monoclonal cell population.
The expression of the fusion protein was detected on western blot by incubating with antibody against CSPP-L. The antibody detected both the fusion protein and endogenous protein in cells.

5.1.1 Localization of fusion protein

Antibody against CEP131 was used as a reference marker for Centriolar satellites and antibody against the FLAG protein was used to detect the fusion protein. Localization of the fusion protein to the centriolar satellites was confirmed by fluorescence microscopy. Localization of the fusion protein during mitosis was also studied. Cells were incubated with biotin for 10 minutes, stained with antibody against the FLAG protein and antibody against EB3. Localization of the fusion protein during mitosis was difficult to detect, but biotinylated proteins were better detected and had same localization pattern as the CSPP-L protein during mitosis (49).

These data indicated that the miniTurbo-CSPPL-fusion protein resembled the expected localization pattern in proliferating/cycling cells. We examined next the localization pattern of miniTurboID-CSPP-L in respone to serum starvation, where endogenous CSPP-L localizes to the cilia axoneme and its tip region. An antibody against ARL13B was used to stain the ciliary membrane. An antibody against the FLAG protein was used for staining of the fusion protein. The fusion protein localized to the basal body and satellites around the cilium, but unexpectedly, was undetectable on the ciliary axoneme in two indendent experiments. A reason for the missing localization of the fusion protein on the cilia could be a conformational change or complexation of the ciliary (microtubule associated) fusion protein, which prevents the antibody from binding to the FLAG. In this experiment, cells were fixed with methanol before staining with antibody, perhaps using a different fixation solution or a pre-extraction protocol as used in a different study can give a

better result (61). However, we cannot exclude the possibility that the fusion protein does not have the same localization pattern in ciliated cells as documented for the endogenous CSPP-L protein, i.e. that the N-terminal BirA*-FLAG tag perturbs the functionality of the fusion protein. Cilia frequency for the generated cell lines was investigated by counting ciliated cells and non-ciliated cells and comparing the mean of the experiments with the parental, untransduced hTERT-RPE1 cell line (the control cell line). A reduced ciliation frequency in the selected in the selected monoclonal cell line was observed. As only a single clone was examined, we cannot distinguish if the reduced ciliation capacity is caused by the integration event, the expression of the fusion protein, or a previously acquired inert property of this particular clone.

5.1.2 Biotinylation assay

Generated cell lines were added biotin in the timeframes of 5 minutes, 10 minutes, 15 minutes and 30 minutes. The timeframes were selected based on a former study revealing the short biotinylation timeframe of miniTurboID (55). Cells were studied by fluorescence microscopy. Biotinylation of proteins was seen in all timeframes. Some low and diffusebackground staining with biotin was also observed, but did not increase over time and was similar in non-transduced control cells. The co-localization of biotinylated proteins and the miniTurbo-FLAG-CSPP-L fusion protein in cycling cells indicated site-specific modification of the CSPP-L proxymitome. A similar examination in serum-starved ciliated cells remains to be performed. An initial evaluation of biotinylation efficacy by Western blot analysis of total cell lysates from polyclonal cell lines failed to detect biotinylated proteins using HRP-conjugated streptavidin (data not shown). It was thought that maybe a mixture of both transfected and non-transfected cells could be the reason for the lack of extracted biotinylated proteins (figure 4.10). We repeated the experiment in a monoclonal cell line and enriched for biotinylated proteins using a streptavidin resin (figure 4.11). This improved the assay and now more biotinylated proteins were detectable after incubation with HRP-streptavidin. This result is promising for future optimization of preparative labeling experiments. Earlier studies were this experiment has been done resulted in more extracted biotinylated proteins (55).

6. Conclusions

hTERT-RPE1 cells expressing miniTurboID-CSPP-L were generated to study the CSPP-L protein proximity. Localization of the miniTurboID-CSPP-L protein and its biotinylation activity was characterized on immunofluorescence microscopy. The localization of the fusion protein to the centrosome, Centriolar satelittes and mitotic spindle apparatus was confirmed, resembling the localization pattern of endogenous CSPP-L. The localization of the fusion protein to primary cilia (unfortunately) remains however uncertain.

7. Future studies

We successfully created cell line that can be used to study the proximal proteins of CSPP-L in different stages of the cell cycle by addition of biotin, extraction of biotinylated proteins from cell lysates, and their identification by mass spectrometry. However, localization of the fusion protein in ciliated cells needs to be further investigated. Preferably further individual clones should be isolated to evaluate a potential dominant negative effect of the fusion protein on cilia formation. Further, different pre-extraction and fixation conditions may be tested to study if lack of accessibility of the FLAG-epitope may underlie poor detection of the CSPP-L fusion protein at the cilia axoneme. Different incubation times with varying concentrations of biotin may also be tested in serum starved cells to examine if proteins of the primary cilium are biotinylated (indirect evidence for localization). Also the fusion of the miniTurboID tag to the C-terminal end should be tested. Transduction of CSPP1-/- hTERT-RPE1 cells with these virusconstructs may also be considered, to test if the fusion proteins can rescue the ciliation defect in this cell line. Secondly, the extraction of the biotinylated proteins should also be further investigated. A methodological approach for this can be to increase the concentration of protein lysates by increasing the number of cells in the experiment, and to test other lysis conditions for isolation the biotinylated proteins (eg change to RIPA buffer, including sonication).

REFERENCES

1. Arslanhan MD, Gulensoy D, Firat-Karalar EN. A Proximity Mapping Journey into the Biology of the Mammalian Centrosome/Cilium Complex. Cells. 2020;9(6).
2. Sonnen KF, Schermelleh L, Leonhardt H, Nigg EA. 3D-structured illumination microscopy provides novel insight into architecture of human centrosomes. Biol Open. 2012;1(10):965-76.
3. Arquint C, Gabryjonczyk AM, Nigg EA. Centrosomes as signalling centres. Philos Trans R Soc Lond B Biol Sci. 2014;369(1650).
4. Wang JT, Stearns T. The ABCs of Centriole Architecture: The Form and Function of Triplet Microtubules. Cold Spring Harb Symp Quant Biol. 2017;82:145-55.
5. Firat-Karalar EN, Stearns T. The centriole duplication cycle. Philos Trans R Soc Lond B Biol Sci. 2014;369(1650).
6. Mardin BR, Schiebel E. Breaking the ties that bind: new advances in centrosome biology. J Cell Biol. 2012;197(1):11-8.
7. Bettencourt-Dias M, Glover DM. Centrosome biogenesis and function: centrosomics brings new understanding. Nat Rev Mol Cell Biol. 2007;8(6):451-63.
8. Nam HJ, Naylor RM, van Deursen JM. Centrosome dynamics as a source of chromosomal instability. Trends Cell Biol. 2015;25(2):65-73.
9. de Forges H, Bouissou A, Perez F. Interplay between microtubule dynamics and intracellular organization. Int J Biochem Cell Biol. 2012;44(2):266-74.
10. Etienne-Manneville S. From signaling pathways to microtubule dynamics: the key players. Curr Opin Cell Biol. 2010;22(1):104-11.
11. Tovey CA, Conduit PT. Microtubule nucleation by gamma-tubulin complexes and beyond. Essays Biochem. 2018;62(6):765-80.
12. Akhmanova A, Steinmetz MO. Control of microtubule organization and dynamics: two ends in the limelight. Nat Rev Mol Cell Biol. 2015;16(12):711-26.
13. Garcin C, Straube A. Microtubules in cell migration. Essays Biochem. 2019;63(5):509-20.
14. Barenz F, Mayilo D, Gruss OJ. Centriolar satellites: busy orbits around the centrosome. Eur J Cell Biol. 2011;90(12):983-9.
15. Odabasi E, Batman U, Firat-Karalar EN. Unraveling the mysteries of centriolar satellites: time to rewrite the textbooks about the centrosome/cilium complex. Mol Biol Cell. 2020;31(9):866-72.
16. Tollenaere MA, Mailand N, Bekker-Jensen S. Centriolar satellites: key mediators of centrosome functions. Cell Mol Life Sci. 2015;72(1):11-23.
17. Hori A, Toda T. Regulation of centriolar satellite integrity and its physiology. Cell Mol Life Sci. 2017;74(2):213-29.
18. Gheiratmand L, Coyaud E, Gupta GD, Laurent EM, Hasegan M, Prosser SL, et al. Spatial and proteomic profiling reveals centrosome-independent features of centriolar satellites. EMBO J. 2019;38(14):e101109.
19. Prosser SL, Pelletier L. Centriolar satellite biogenesis and function in vertebrate cells. J Cell Sci. 2020;133(1).
20. Conkar D, Bayraktar H, Firat-Karalar EN. Centrosomal and ciliary targeting of CCDC66 requires cooperative action of centriolar satellites, microtubules and molecular motors. Sci Rep. 2019;9(1):14250.
21. Wei Q, Ling K, Hu J. The essential roles of transition fibers in the context of cilia. Curr Opin Cell Biol. 2015;35:98-105.

22. Pedersen LB, Mogensen JB, Christensen ST. Endocytic Control of Cellular Signaling at the Primary Cilium. Trends Biochem Sci. 2016;41(9):784-97.
23. Brown JM, Witman GB. Cilia and Diseases. Bioscience. 2014;64(12):1126-37.
24. Anvarian Z, Mykytyn K, Mukhopadhyay S, Pedersen LB, Christensen ST. Cellular signalling by primary cilia in development, organ function and disease. Nat Rev Nephrol. 2019;15(4):199-219.
25. Nachury MV, Seeley ES, Jin H. Trafficking to the ciliary membrane: how to get across the periciliary diffusion barrier? Annu Rev Cell Dev Biol. 2010;26:59-87.
26. Goncalves J, Pelletier L. The Ciliary Transition Zone: Finding the Pieces and Assembling the Gate. Mol Cells. 2017;40(4):243-53.
27. Latour BL, Van De Weghe JC, Rusterholz TD, Letteboer SJ, Gomez A, Shaheen R, et al. Dysfunction of the ciliary ARMC9/TOGARAM1 protein module causes Joubert syndrome. J Clin Invest. 2020;130(8):4423-39.
28. Conkar D, Firat-Karalar EN. Microtubule-associated proteins and emerging links to primary cilium structure, assembly, maintenance, and disassembly. FEBS J. 2021;288(3):786-98.
29. Taschner M, Lorentzen E. The Intraflagellar Transport Machinery. Cold Spring Harb Perspect Biol. 2016;8(10).
30. He M, Agbu S, Anderson KV. Microtubule Motors Drive Hedgehog Signaling in Primary Cilia. Trends Cell Biol. 2017;27(2):110-25.
31. Izawa I, Goto H, Kasahara K, Inagaki M. Current topics of functional links between primary cilia and cell cycle. Cilia. 2015;4:12.
32. Sanchez I, Dynlacht BD. Cilium assembly and disassembly. Nat Cell Biol. 2016;18(7):711-7.
33. Garcia-Gonzalo FR, Reiter JF. Open Sesame: How Transition Fibers and the Transition Zone Control Ciliary Composition. Cold Spring Harb Perspect Biol. 2017;9(2).
34. Shakya S, Westlake CJ. Recent advances in understanding assembly of the primary cilium membrane. Fac Rev. 2021;10:16.
35. Lu Q, Insinna C, Ott C, Stauffer J, Pintado PA, Rahajeng J, et al. Early steps in primary cilium assembly require EHD1/EHD3-dependent ciliary vesicle formation. Nat Cell Biol. 2015;17(3):228-40.
36. Breslow DK, Holland AJ. Mechanism and Regulation of Centriole and Cilium Biogenesis. Annu Rev Biochem. 2019;88:691-724.
37. Bernabe-Rubio M, Alonso MA. Routes and machinery of primary cilium biogenesis. Cell Mol Life Sci. 2017;74(22):4077-95.
38. Goetz SC, Liem KF, Jr., Anderson KV. The spinocerebellar ataxia-associated gene Tau tubulin kinase 2 controls the initiation of ciliogenesis. Cell. 2012;151(4):847-58.
39. Cajanek L, Nigg EA. Cep164 triggers ciliogenesis by recruiting Tau tubulin kinase 2 to the mother centriole. Proc Natl Acad Sci U S A. 2014;111(28):E2841-50.
40. Avasthi P, Marshall WF. Stages of ciliogenesis and regulation of ciliary length. Differentiation. 2012;83(2):S30-42.
41. Reiter JF, Leroux MR. Genes and molecular pathways underpinning ciliopathies. Nat Rev Mol Cell Biol. 2017;18(9):533-47.
42. Brancati F, Dallapiccola B, Valente EM. Joubert Syndrome and related disorders. Orphanet J Rare Dis. 2010;5:20.
43. Parisi MA. The molecular genetics of Joubert syndrome and related ciliopathies: The challenges of genetic and phenotypic heterogeneity. Transl Sci Rare Dis. 2019;4(1-2):25-49.

44. Yang TT, Su J, Wang WJ, Craige B, Witman GB, Tsou MF, et al. Superresolution Pattern Recognition Reveals the Architectural Map of the Ciliary Transition Zone. Sci Rep. 2015;5:14096.
45. Akizu N, Silhavy JL, Rosti RO, Scott E, Fenstermaker AG, Schroth J, et al. Mutations in CSPP1 lead to classical Joubert syndrome. Am J Hum Genet. 2014;94(1):80-6.
46. Tuz K, Bachmann-Gagescu R, O'Day DR, Hua K, Isabella CR, Phelps IG, et al. Mutations in CSPP1 cause primary cilia abnormalities and Joubert syndrome with or without Jeune asphyxiating thoracic dystrophy. Am J Hum Genet. 2014;94(1):62-72.
47. Patzke S, Stokke T, Aasheim HC. CSPP and CSPP-L associate with centrosomes and microtubules and differently affect microtubule organization. J Cell Physiol. 2006;209(1):199-210.
48. Patzke S, Hauge H, Sioud M, Finne EF, Sivertsen EA, Delabie J, et al. Identification of a novel centrosome/microtubule-associated coiled-coil protein involved in cell-cycle progression and spindle organization. Oncogene. 2005;24(7):1159-73.
49. Patzke S, Redick S, Warsame A, Murga-Zamalloa CA, Khanna H, Doxsey S, et al. CSPP is a ciliary protein interacting with Nephrocystin 8 and required for cilia formation. Mol Biol Cell. 2010;21(15):2555-67.
50. Frikstad KM, Molinari E, Thoresen M, Ramsbottom SA, Hughes F, Letteboer SJF, et al. A CEP104-CSPP1 Complex Is Required for Formation of Primary Cilia Competent in Hedgehog Signaling. Cell Rep. 2019;28(7):1907-22 e6.
51. Sternemalm J, Russnes HG, Zhao X, Risberg B, Nord S, Caldas C, et al. Nuclear CSPP1 expression defined subtypes of basal-like breast cancer. Br J Cancer. 2014;111(2):326-38.
52. Asiedu M, Wu D, Matsumura F, Wei Q. Centrosome/spindle pole-associated protein regulates cytokinesis via promoting the recruitment of MyoGEF to the central spindle. Mol Biol Cell. 2009;20(5):1428-40.
53. Roux KJ, Kim DI, Burke B. BioID: a screen for protein-protein interactions. Curr Protoc Protein Sci. 2013;74:19 23 1-19 23 14.
54. Firat-Karalar EN. Proximity mapping of the microtubule plus-end tracking protein SLAIN2 using the BioID approach. Turk J Biol. 2020;44(2):61-72.
55. Branon TC, Bosch JA, Sanchez AD, Udeshi ND, Svinkina T, Carr SA, et al. Efficient proximity labeling in living cells and organisms with TurboID. Nat Biotechnol. 2018;36(9):880-7.
56. Firat-Karalar EN, Stearns T. Probing mammalian centrosome structure using BioID proximity-dependent biotinylation. Methods Cell Biol. 2015;129:153-70.
57. Roux KJ, Kim DI, Raida M, Burke B. A promiscuous biotin ligase fusion protein identifies proximal and interacting proteins in mammalian cells. J Cell Biol. 2012;196(6):801-10.
58. May DG, Scott KL, Campos AR, Roux KJ. Comparative Application of BioID and TurboID for Protein-Proximity Biotinylation. Cells. 2020;9(5).
59. Gupta GD, Coyaud E, Goncalves J, Mojarad BA, Liu Y, Wu Q, et al. A Dynamic Protein Interaction Landscape of the Human Centrosome-Cilium Interface. Cell. 2015;163(6):1484-99.
60. Quarantotti V, Chen JX, Tischer J, Gonzalez Tejedo C, Papachristou EK, D'Santos CS, et al. Centriolar satellites are acentriolar assemblies of centrosomal proteins. EMBO J. 2019;38(14):e101082.
61. Hua K, Ferland RJ. Fixation methods can differentially affect ciliary protein immunolabeling. Cilia. 2017;6:5.

APPENDIX

A1 Reagents

Table 4: List of reagents used in this master thesis, listed in alphabetic order

Product	**Manufactured**	**Product number**
4-15% Mini-PROTEAN® TGX™ Precast Protein Gels, 15-well, 15 µl	Bio-Rad	4561086
50x Tris/Acetic Acid/EDTA (TAE), Nucleic Acid Electrophoresis Buffer	Bio-Rad Laboratories AB	1610743
Ampicillin	Sigma-Aldrich	A5354
Blasticidin	InvivoGen	Ant-bl-1
Bovine Serum Albumin	Sigma-Aldrich	A3059
cOmplete™ Protease Inhibitor Cocktail	Sigma-Aldrich	04693116001
Cutsmart® Buffer	New England BioLabs	B7204S
Dimethyl sulfoxide	Sigma-Aldrich	41639
Dulbecco´s Modified Eagle Medium	ThermoFisher Scientific	31966-021
Dulbecco´s Modified Eagle Medium: Nutrient mixture F-12	ThermoFisher Scientific	31331-028
Dulbecco's phosphate buffered saline	Sigma-Aldrich	D8537
EcoRI	New England BioLabs	R0101L
Fetal Bovine Serum	ThermoFisher Scientific	16000044
Gateway™ LR Clonase™ II Enzyme mix	ThermoFisher Scientific	11791020
Gel Loading Dye, Purple (6X)	New England	B7024S

	BioLabs	
GeneJET Gel Extraction Kit	ThermoFisher Scientific	K0692
Hoechst 33258	Sigma-Aldrich	861405
hTERT-RPE1	Clontech	-
Kanamycin	Sigma-Aldrich	K0254
LentiX	Invitrogen	-
Lipofectamine™ 3000 Transfection Reagent	ThermoFisher Scientific	L3000015
Mix & Go! Competent Cells-Zymo 10B	Zymo Research	T3020
Micro tubes 1,5 ml	Sarstedt	-
NEBuilder HiFi DNA Assembly Master Mix	New England BioLabs	E2621
NheI-HF	New England BioLabs	R3131L
NucleoSpin Plasmid, Mini kit for plasmid DNA	Macherey-Nagel	740588.250
Opti-MEM™ I Reduced Serum Medium	ThermoFisher Scientific	31985070
Penicillin-Streptomycin	Sigma-Aldrich	P4333
Phosphatase Inhibitor Cocktail 2	Sigma-Aldrich	P5726-5ml
Pierce™ Biotin	ThermoFisher Scientific	29129
Pierce™ High Capacity Streptavidin Agarose	ThermoFisher Scientific	20357
Poly-L-lysine	Sigma-Aldrich	P7890-100
ProLong Gold Antifade Reagent	Invitrogen	P36930
Running buffer 10x Tris/Glycine/SDS	Bio-Rad	161-0772
SalI	New England	R0138L

	BioLabs	
Skim milk powder	Sigma-Aldrich	70166
Supersignal™ West Dura Extended Duration Substrate	ThermoFisher Scientific	34075
Supersignal™ West Pico PLUS Chemiluminescent Substrat	ThermoFisher Scientific	34579
T25 cell flasks	ThermoFisher Scientific	156367
T75 cell flasks	ThermoFisher Scientific	156499
Trans-Blot Turbo Mini-size Transfer stacks	Bio-Rad	10025915
Trans-Blot Turbo 5x Transfer Buffer	Bio-Rad	10026938
Tris Buffered Saline with Tween 20:5L of 20X	Santa Cruz	Sc-362311
Trypsin-EDTA solution	Sigma-Aldrich	T3924
UltraPure™ Agarose (100g)	ThermoFisher Scientific	16500100
XhoI	New England BioLabs	R0146L
ZymoPURE II Plasmid Midiprep Kit	Zymo Research	D4200

Table 5: List of instruments/equipment used in the master thesis

Instruments / Equipment	**Manufactured**
Beckman Counter Z2	Beckman Coulter Life Sciences
NanoDrop 2000 Spectrophotometer	ThermoFisher Scientific
CellObserver Microscope System	Carl Zeiss
Trans-Blot Turbo Transfer System	Bio-Rad
MJ Research PTC-100 Thermal Cycler	Marshall Scientific
Eppendorf™ ThermoMixer Temperature Control Device	Fisher Scientific
Hettich – MIKRO 20	Hettich
Multitron standard, incubator shaker for microbial applications	Infors HT
Screw cap tube, 50 ml, (LxØ)	Sarstedt
Cell Scrapers	Sarstedt
Original-Perfusor® Syringe 20 ml	BBraun

Sequencing primer:

>pENTR220univF#5

cggttatccacagaatcaggg

A2 Solutions

Transfer buffer:

-200 ml 5x Transfer Buffer

-600 ml MQH_2O

-200 ml Ethanol

2x Sample loading buffer (SLB):

- 4 ml 10% SDS solution
- 2 ml Glycerol
- 1 ml 0,1% Bromophenol blue
- 2,5 ml 9,5 M TrisCl pH 6,8
- 0,5 ml dithiothreitol/ß-mercaptoethanol

Lysis buffer:

- 10 ml 1M Hepes, pH 7
- 10 ml 5M NaCl
- 2 ml 0,5 M EDTA, pH 8,5
- 200 µl NP-40
- 20 ml glycerol
- 157,3 ml MQH_2O

Biotin solution:

2 mg Biotin was dissolved in 1 ml of DMSO to make a 50 mM biotin stock solution.

A3 Primary and secondary antibodies

Table 6: List of primary antibodies used in the master thesis.

Usage	**Antibody**	**Antibody host**	**Dilution**	**Producer**	**Product number**
WB	Anti-CSPP-1	Rabbit polyclonal	1:1000	Proteintech	11931-1-AP
IF	Anti-CEP131	Rabbit polyclonal	1:500	Abcam	Ab99379
IF	FLAGM2	Mouse monoclonal	1:500	Sigma-Aldrich	F3165-2MG
IF	Anti-EB3	Rat monoclonal	1:500	Sigma-Aldrich	A6066
IF	Anti-ARL13B	Rabbit polyclonal	1:500	Proteintech	17711-1-AP

Table 7: List of secondary antibodies used in the master thesis

Antibody/Label	**Dilution**	**Producer**	**Product number**
HRP-streptavidin	1:2000	Cell Signaling Technology	3999
FITC-streptavidin	1:500	BD Biosciences	554060
Goat Anti-rabbit (GAR) IgG with T-phycoerythrin	1:10000	ThermoFisher Scientific	K0692
Donkey-anti-mouse – Cy3	1:1000	Jackson Immuno Research Labs	715-165-150
Donkey-anti-rabbit-AlexaFluor 647	1:1000	Jackson Immuno Research Labs	711-605-152